Multiphoton-scattering theory and generalized master equations

Tao Shi,[1] Darrick E. Chang,[2] and J. Ignacio Cirac[1]

[1]*Max-Planck-Institut für Quantenoptik, Hans-Kopfermann-Strasse 1, 85748 Garching, Germany*
[2]*ICFO-Institut de Ciencies Fotoniques, Mediterranean Technology Park, 08860 Castelldefels (Barcelona), Spain*

We develop a scattering theory to investigate the multiphoton transmission in a one-dimensional waveguide in the presence of quantum emitters. It is based on a path integral formalism, uses displacement transformations, and does not require the Markov approximation. We obtain the full time evolution of the global system, including the emitters and the photonic field. Our theory allows us to compute the transition amplitude between arbitrary initial and final states, as well as the S matrix of the asymptotic in and out states. For the case of few incident photons in the waveguide, we also rederive a generalized master equation in the Markov limit. We compare the predictions of the developed scattering theory and that with the Markov approximation. We illustrate our methods with five examples of few-photon scattering: (i) by a two-level emitter, (ii) in the Jaynes-Cummings model; (iii) by an array of two-level emitters; (iv) by a two-level emitter in the half-end waveguide; and (v) by an array of atoms coupled to Rydberg levels. In the first two, we show the application of the scattering theory in the photon scattering by a single emitter, and examine the correctness of our theory with the well-known results. In the third example, we analyze the condition of the Markov approximation for the photon scattering in the array of emitters. In the fourth one, we show how a quantum emitter can generate entanglement of outgoing photons. Finally, we highlight the interplay between the phenomenon of electromagnetic-induced transparency and the Rydberg interaction, and show how this results in a rich variety of possibilities in the quantum statistics of the scattering photons.

I. INTRODUCTION

The exploration of quantum optical systems characterized by strong photon-photon interactions has inspired a lot of research and extensive studies recently [1–4]. Those systems provide us with a versatile platform to investigate the generation [5] and transport of nonclassical light, as well as the behavior of single-photon sources [6–8] and switches [3,9–12]. Those are the basic ingredients in quantum-optical [13] and quantum information devices [14,15].

The manipulation of nonclassical light typically requires devices displaying either strong nonlinearities [4], or quantum interference effects [16,17]. Among many other phenomena, they give rise to peculiar quantum statistical behavior of the emitted or scattered photons, like antibunching [18] in the generation of single photons or photon pairs [19,20]. Such devices are being investigated in different incarnations, including cavity QED [1,2,16,17,21–25], solid state [6,8,26–29], and circuit QED systems [30,31]. At the many-particle level, the strong interaction between the nonlinear devices and the photons results in the generation of many-body states, which can be studied in terms of dissipative versions of quantum spin models [32]. In particular, the investigations of the atomic steady state and the photon transmission properties reveal a rich variety of quantum phases [33–37] and photon statistics [38].

In order to characterize how atomic (or any other) nonlinear devices can be used to create and manipulate photonic states, one can analyze the transmission spectra and the photon statistics, for instance, in terms of the second order correlation function of the photons emitted under the presence of weak driving light. This analysis is typically addressed through an input-output theory relating the correlation functions of the emitted photons to those of the atomic system in steady state [18]. Those can be determined using a master equation approach, based on the Born-Markov approximation. This approach has proven to be very successful in most of the experimentally relevant situations. Even though that is a very good approximation for most models in quantum optics, in the presence of several emitters [39], or in certain regimes its use may not be justified.

In order to analyze the transmission properties exactly, several elegant approaches [21,22,40–49] have been developed for the few-photon scattering process, where the Born-Markov approximation is not involved. The exact analysis of single- and two-photon transmissions was first addressed through the Bethe ansatz approach [21], which is equivalent to the Lippmann-Schwinger scattering theory. This approach establishes the exact scattering matrix (S matrix) between the in and out asymptotic states of photons, which determines the transmission spectrum and the second order correlation function of outgoing photons. It turns out that the Bethe ansatz approach is very successful in the two-photon scattering by a single emitter with simple structure, e.g., the two-level emitter; however, the generalization to the photon transmission by several emitters is difficult. The approach [40] based on the input-output theory is able to provide the exact S matrix for the two-photon scattering by two emitters. Here, since a closed set of motion equations for emitter operators are required, the exact S matrix can only be obtained in some very limited cases, e.g., two emitters with simple structures.

The systematic approach to the exact S matrix in the multiphoton scattering process is based on quantum field theory. Through either the Lehmann-Symanzik-Zimmerman reduction formalism [22] or the input-output theory, the exact S matrix is related to the time ordered correlation function of emitter operators, which can be obtained by the functional

integration of the photonic bath modes. The functional integration provides an efficient approach to analyze the photon statistical properties in the multiphoton scattering by emitters with complicated structures, e.g., the Jaynes-Cummings (JC) system [23] and the atom-coupled whispering gallery resonator [25]. However, the exact S matrix is only able to describe the evolution of photonic bath in the asymptotic limit, thus, it fails to depict the transient dynamics of emitters, e.g., the single-photon detection in the superconducting edge sensor [50–52]. Recently, a generalized input-output theory [42] was established by the subtle combination of the input-output theory and the quantum regression theorem, which allowed us to investigate both the transient dynamics and the photon statistics in the asymptotic limit. Here, a generalized master equation is obtained to describe the transient dynamics of several emitters under the presence of few incident photons. The generalized input-output theory and master equation involve the Markov approximation, thus, they are not able to provide the exact results. The use of the Markov approximation in the presence of several emitters needs to be justified.

In this paper, based on the path integral formalism, we develop the scattering theory to characterize the full time evolution of the global system (including the emitters and the photonic bath) exactly for the few-photon scattering by several emitters with complicated structures. Our theory provides the transition amplitudes from the arbitrary initial state to the corresponding final state without the Markov approximation, where both the quantum statistics of scattering photons and the transient dynamics of emitters can be analyzed exactly. In the Markovian limit, the exact results from our theory perfectly agree with those from the quantum regression approach, which justifies the validity of the Markov approximation. Similarly, the generalized master equation is reproduced to describe the dynamics of emitters in the presence of few incident photons. Here, we emphasize that the generalized master equation establishes the close relation between the properties of photons emitted under the presence of weak driving light and those in the few-photon scattering by the emitters.

Using the two paradigmatic examples, i.e., the few-photon transmission to the two-level emitter and the JC system, we examine the correctness of our theory in the photon scattering by the single emitter. Here, the developed scattering theory reproduces the well-known results [21–23,53] for the transmission spectra and the second order correlation function. For the few-photon scattering by several emitters, we investigate the condition of the Markov approximation in detail. In particular, we show that the Markov approximation is valid under certain conditions relating the bandwidth of the dynamics and the distance of separation between emitters. In the non-Markovian regime, the exact results exhibit peculiar features associated with retardation of pulses between emitters.

By the developed scattering theory, we explore some novel phenomena in two new situations. For the photon scattering by a single two-level emitter in the half-end waveguide, we show how the two-level emitter can generate entanglement of outgoing photons. For the photon transmission in the array of atoms under conditions of electromagnetically induced transparency (EIT) [54] and coupled to Rydberg levels, we highlight the EIT phenomenon and the Rydberg interaction. Here, the second order correlation functions of emitted pho-

tons, the co-propagation of dark polaritons, and the collision of the counterpropagating polaritons in the transient process are analyzed, which show a rich variety of the quantum statistics of photons and Rydberg excitations. The developed scattering theory is proven to be a very efficient and systematical approach to investigate the quantum statistics of photons in the array of the interacting emitters with complicated structures.

The paper is organized as follows. In Sec. II, the five models are introduced, which are the two-level emitter and the JC system coupled to the photonic waveguide, the two-level emitter in the half-end waveguide, and the photon scattering by an array of two-level atoms and EIT atoms coupled to Rydberg levels. In Sec. III, the developed scattering theory is established, where the exact S matrix relates the asymptotic incident and final states. For the transient process, the generalized master equation is derived to characterize the time evolution of the quantum emitters. In Sec. IV, two paradigmatic examples, i.e., the photon transmission to the two-level emitter and the JC system, are used to examine our theory and illustrate how our method works in the photon scattering by the single emitter. In Sec. V, we analyze the validity of the Markov approximation for the photon scattering by several emitters. In Sec. VI, we show the generation of entanglement between two scattering photons by a single two-level emitter in the half-end waveguide. In Sec. VII, the photon transmission to an array of EIT atoms coupled to Rdyberg levels is investigated. In Sec. VIII, the results are summarized with the outlook.

II. SCATTERING MODELS

In this section, we introduce the models we are going to use in order to investigate the transmission of waveguide photons interacting with quantum systems. Those could be single emitters (e.g., a multilevel atom [3,12,21,22,46,55], an atom coupled to a cavity mode [1,2]), or an array of emitters coupled, for instance, to Rydberg levels [42,56].

The model Hamiltonian has the form $H = H_{\rm w} + H_{\rm sys} + H_{\Gamma} + H_{\Gamma_f}$ and contains four parts: (a) The free propagation of photons in the waveguide is described by the Hamiltonian

$$H_{\rm w} = \sum_k [(k_0 + k) r_k^\dagger r_k + (k_0 - k) l_k^\dagger l_k], \quad (1)$$

where r_k ($r_k^\dagger$) and l_k ($l_k^\dagger$) are the annihilation (creation) operators for the right- and left-moving modes with the central frequency k_0 in the waveguide. (b) The system Hamiltonian $H_{\rm sys}$ describes the quantum emitters, and will be explicitly given later for different examples. (c) The interaction between the waveguide photons and the emitters is given by the Hamiltonian

$$H_{\Gamma} = \sum_i [\sqrt{\Gamma_{r,i}} r^\dagger(x_i) + \sqrt{\Gamma_{l,i}} l^\dagger(x_i)] O_i + {\rm H.c.}, \quad (2)$$

where the left- and right-moving photon fields $r(x_i) = \sum_k r_k e^{i(k+k_0)x_i}/\sqrt{L}$ and $l(x_i) = \sum_k l_k e^{i(k-k_0)x_i}/\sqrt{L}$ couple to the operator O_i of the ith emitter at the position x_i with coupling strengths $\Gamma_{r(l),i}^{1/2}$. In momentum space, the interaction
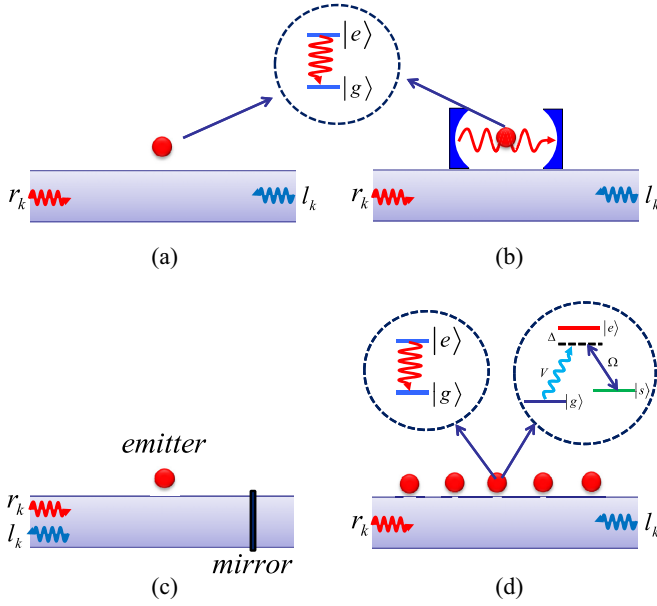
FIG. 1. (Color online) Four examples of the problem studied here: (a) single two-level system coupled to a waveguide; (b) JC system coupled to a waveguide; (c) single two-level system coupled to a one-sided waveguide; and (d) an array of atoms coupled to a waveguide.

Hamiltonian reads

$$H_\Gamma = \sum_k (r_k^\dagger O_{k,+} + l_k^\dagger O_{k,-}) + \text{H.c.}, \qquad (3)$$

where the collective operators $O_{k,\pm} = \sum_i \sqrt{\Gamma_i} O_i e^{-i(k\pm k_0)x_i}/\sqrt{L}$, and we focus on the symmetric coupling case, i.e., $\Gamma_{r,i} = \Gamma_{l,i} \equiv \Gamma_i$. Without loss of generality, we choose the position of the first emitter $i = 1$ at the origin $x_1 = 0$. (d) Apart from the decay to the waveguide, there may exist other decay channels to free space (spontaneous emission outside the waveguide). We describe this through the Hamiltonian H_{Γ_f}. Here, each emitter couples to some system operator $\tilde{O}_i$ with a JC-type coupling (2).

We now present some relevant examples for the system Hamiltonian H_{sys}, and which will be analyzed in detail in the following sections. As shown in Fig. 1(a), the simplest example consists of a two-level system with the energy level spacing $\omega_e = k_0$ between states $|e\rangle$ and $|g\rangle$. The Hamiltonian is $H_{\text{sys}} = \omega_e |e\rangle\langle e|$ and $O_{i=1} = \tilde{O}_i = O = \tilde{O} = |g\rangle\langle e|$.

The second example is the JC system shown in Fig. 1(b). The Hamiltonian

$$H_{\text{sys}} = \omega_c a^\dagger a + \omega_e |e\rangle\langle e| + g(a^\dagger |g\rangle\langle e| + \text{H.c.}) \qquad (4)$$

describes a single two-level system, with the energy level spacing ω_e, coupled to a cavity mode of frequency ω_c. The annihilation operator a corresponds to the cavity mode, and the coupling constant is g. Here, the cavity mode directly couples to the waveguide, i.e., $O_{i=1} = O = a$. The excitations of the cavity field and the two-level system can decay into free space; thus, $\tilde{O}_i$ would be a and $|g\rangle\langle e|$.

We analyze the validity of the Markov approximation and the retardation effect using the third example. Here, as shown in Fig. 1(d), the waveguide photons couple to an array of

two-level emitters with frequency $\omega_e = k_0$ and lattice spacing d. The emitter Hamiltonian is

$$H_{\text{sys}} = \sum_i \left(\omega_e b_i^\dagger b_i + \tfrac{1}{2} U_0 b_i^\dagger b_i^\dagger b_i b_i\right), \qquad (5)$$

where the hardcore boson b_i is introduced to describe a two-level emitter, and the hardcore behavior is obtained in the limit $U_0 \to \infty$. The waveguide photons couple to the collective modes $O_{k,\pm} = \sqrt{\Gamma/L} \sum_i e^{-i(k\pm k_0)x_i} b_i$, where the decay rates $\Gamma_{r(l),i}$ are taken to be the constant $\Gamma_{r(l),i} = \Gamma$. The excitation decays into the free space, i.e., $\tilde{O}_i = b_i$.

The fourth example is a single emitter in front of a mirror, as shown in Fig. 1(c). The system Hamiltonian is $H_{\text{sys}} = H_{\text{emitter}} + \omega_b b^\dagger b$, and the collective operators are

$$O_{k,+} = \sqrt{\frac{\Gamma}{L}} O e^{-i(k+k_0)x_0} + \sqrt{\frac{\Gamma_b}{L}} b,$$
$$O_{k,-} = \sqrt{\frac{\Gamma}{L}} O e^{-i(k-k_0)x_0} + \sqrt{\frac{\Gamma_b}{L}} b, \qquad (6)$$

where the boson mode b is introduced to describe the mirror in the limit $\Gamma_b \to \infty$. The decay of the emitter excitation into free space is characterized by $\tilde{O}_i = |g\rangle\langle e|$.

The fifth example is an array of EIT atoms coupled to Rydberg levels, with lattice spacing d, as is schematically shown in Fig. 1(d). The emitter Hamiltonian is

$$H_{\text{sys}} = \sum_i [\omega_e e_i^\dagger e_i + \omega_s s_i^\dagger s_i + (\Omega e^{-i\omega_d t} e_i^\dagger s_i + \text{H.c.})]$$
$$+ H_{\text{HC}} + \frac{1}{2} \sum_{ij} U_{ij} s_i^\dagger s_j^\dagger s_j s_i. \qquad (7)$$

Here, we use hardcore bosons e and s to describe a Rydberg-EIT atom. There are three atomic levels: the ground state $|g\rangle$, the excited state $|e\rangle$ with frequency ω_e, and the Rydberg state $|s\rangle$ with frequency ω_s. The hardcore behavior is obtained through

$$H_{\text{HC}} = \frac{U_0}{2} \sum_i (e_i^\dagger e_i + s_i^\dagger s_i)(e_i^\dagger e_i + s_i^\dagger s_i - 1) \qquad (8)$$

in the limit $U_0 \to \infty$, which projects out the states $|ee\rangle$, $|es\rangle$, and $|ss\rangle$ of each atom with double occupations. The atoms in the Rydberg state $|s\rangle$ experience long-range interactions, U_{ij}, [57]. For instance, we can take the van der Waals interaction $U_{ij} = C_6/|x_i - x_j|^6$, the dipolar interaction $U_{ij} = C_3/|x_i - x_j|^3$, or the uniform interaction $U_{ij} = C_0$ [42]. The transition between states $|e\rangle$ and $|s\rangle$ is induced by a classical field of frequency ω_d and corresponding Rabi frequency Ω. The waveguide photons couple to the collective modes $O_{k,\pm} = \sqrt{\Gamma} \sum_i e^{-i(k\pm k_0)x_i} e_i/\sqrt{L}$, where the decay rates $\Gamma_{r(l),i}$ are taken to be the constant $\Gamma_{r(l),i} = \Gamma$. The e excitations can decay into the free space, i.e., $\tilde{O}_i = e_i$.

For convenience, we transform the Hamiltonian in the rotating frame $r_k \to r_k e^{-ik_0 t}$ and $l_k \to l_k e^{-ik_0 t}$. The system operators are also transformed correspondingly such that the total Hamiltonian is time independent. As a result, in the rotating frame, $H_{\text{w}} = \sum_k k(r_k^\dagger r_k - l_k^\dagger l_k)$, and the frequencies in the system Hamiltonian are replaced by the detunings. This

will be used in the five examples presented in the following sections.

III. GENERAL FORMALISM

In this section, we show the general formalism to study the full dynamics of the global system during the few-photon scattering process. In Secs. III A and III B, we briefly review the results based on the Markov approximation in Ref. [42]. Here, a different method, i.e., the displacement transformation, is introduced to relate the transition amplitude between arbitrary initial and final states with the correlators of emitter operators. Based on the quantum regression theorem, these correlators are obtained by the effective Hamiltonian of the emitters, where the quantum regression theorem requires the Markov approximation. In order to obtain the exact result and examine the validity of the Markov approximation, in Sec. III C we use the path integral formalism to derive the exact transition amplitude, where the non-Markovian effects are taken into account.

In both approaches, the S matrix of the asymptotic in and out states and the transition amplitudes in the transient process are obtained, which agree with each other in the Markov limit. It turns out that for the single emitter coupled to the photon with linear dispersion, the Markovian result is proven to be exact by the path integral approach. For the photon scattering by several emitters, the validity of the Markov approximation is analyzed in Sec. V in detail. In the Markov limit, both approaches give rise to the generalized master equation [42] governing the dynamics of the emitters during the scattering process, where the generalized master equation establishes a close relation between the transient behaviors of emitters in the presence of few incident photons and the dynamics of emitters under the weak driving light.

A. S matrix by quantum regression theorem

In this section, based on the quantum regression theorem, the displacement transformation is used to derive the transition amplitude between arbitrary initial and final states, where the quantum regression theorem involves the Markov approximation.

We introduce the transition amplitude

$$\mathcal{A}(T) = {}_{\rm sys}\langle\varphi_{\rm out}|\langle{\rm out}|e^{-iH(t_f-t_i)}|{\rm in}\rangle|\varphi_{\rm in}\rangle_{\rm sys} \quad (9)$$

from the initial state $|{\rm in}\rangle|\varphi_{\rm in}\rangle_{\rm sys} = |0\rangle_{\rm free}|\psi_{\rm in}\rangle_{\rm w}|\varphi_{\rm in}\rangle_{\rm sys}$ to the final state $|{\rm out}\rangle|\varphi_{\rm out}\rangle_{\rm sys} = |0\rangle_{\rm free}|\psi_{\rm out}\rangle_{\rm w}|\varphi_{\rm out}\rangle_{\rm sys}$ during the time $T = t_f - t_i$. At the instant t_i, the waveguide photons are in the state $|\psi_{\rm in}\rangle_{\rm w}$, and the initial state of the emitters is $|\varphi_{\rm in}\rangle_{\rm sys} = \gamma_{\rm in}^\dagger|G\rangle_{\rm sys}$, where $|G\rangle_{\rm sys}$ and $\gamma_{\rm in}^\dagger$ denote the ground state and some creation operator of the emitters, respectively. Similarly, at the instant t_f, the corresponding final states are $|\varphi_{\rm out}\rangle_{\rm sys} = \gamma_{\rm out}^\dagger|G\rangle_{\rm sys}$ and $|\psi_{\rm out}\rangle_{\rm w}$, respectively. Here, we focus on the transition process without excitations leaking to the free space, and the initial and final states of the free space are the vacuum state $|0\rangle_{\rm free}$.

The initial and final states of waveguide photons can be generally written as

$$|\psi_{\rm in}\rangle_{\rm w} = \sum_{\{n_{k\alpha}\}} \psi_{\rm in}(\{n_{k\alpha}\})\prod_k |n_{k\alpha}\rangle,$$

$$|\psi_{\rm out}\rangle_{\rm w} = \sum_{\{m_{k\alpha}\}} \psi_{\rm out}(\{m_{k\alpha}\})\prod_k |m_{k\alpha}\rangle, \quad (10)$$

where $\{n_{k\alpha}\} = \{n_{k_1\alpha}, n_{k_2\alpha}, \ldots\}$ and $\{m_{k\alpha}\} = \{m_{k_1\alpha}, m_{k_2\alpha}, \ldots\}$ are the number distribution of photons with different momenta k_i in the initial and final states, respectively, and $\alpha = r, l$ denote the right- and left-moving modes. We notice that the relation

$$|n_{k\alpha}\rangle = \lim_{J_{k\alpha}\to 0} \frac{1}{\sqrt{n_{k\alpha}!}} \frac{\partial^{n_{k\alpha}}}{\partial J_{k\alpha}^{n_{k\alpha}}}|J_{k\alpha}\rangle \quad (11)$$

between the Fock state and the unnormalized coherent state $|J_{k\alpha}\rangle = \sum_{n_k} J_{k\alpha}^{n_k}|n_{k\alpha}\rangle/\sqrt{n_{k\alpha}!}$ leads to the coherent representation of the initial and final states

$$|\psi_{\rm in}\rangle_{\rm w} = \mathcal{F}_{\rm in}|\{J_{k\alpha}\}\rangle,$$

$$|\psi_{\rm out}\rangle_{\rm w} = \mathcal{F}_{\rm out}|\{J_{k\alpha}\}\rangle, \quad (12)$$

where

$$\mathcal{F}_{\rm in} = \lim_{\{J_{k\alpha}\}\to 0} \sum_{\{n_{k\alpha}\}} \psi_{\rm in}(\{n_{k\alpha}\})\prod_{k\alpha} \frac{1}{\sqrt{n_{k\alpha}!}} \frac{\delta^{n_{k\alpha}}}{\delta J_{k\alpha}^{n_{k\alpha}}},$$

$$\mathcal{F}_{\rm out} = \lim_{\{J_{k\alpha}\}\to 0} \sum_{\{m_{k\alpha}\}} \psi_{\rm out}(\{m_{k\alpha}\})\prod_{k\alpha} \frac{1}{\sqrt{m_{k\alpha}!}} \frac{\delta^{m_{k\alpha}}}{\delta J_{k\alpha}^{m_{k\alpha}}}. \quad (13)$$

In terms of Eq. (12), the transition amplitude reads

$$\mathcal{A}(T) = \mathcal{F}_{\rm out}^*\mathcal{F}_{\rm in}\mathcal{A}_J(T), \quad (14)$$

where the transition amplitude

$$\mathcal{A}_J(T) = {}_{\rm sys}\langle\varphi_{\rm out}|_{\rm b}\langle\{J_{k\alpha}\}|e^{-iHT}|\{J_{k\alpha}\}\rangle_{\rm b}|\varphi_{\rm in}\rangle_{\rm sys}, \quad (15)$$

and $|\{J_{k\alpha}\}\rangle_{\rm b} = |0\rangle_{\rm free}|\{J_{k\alpha}\}\rangle$. The transition amplitude (15) can be evaluated by either the quantum regression theorem or the path integral approach.

We first show the result from the quantum regression theorem, where the Markov approximation is required. In the interacting picture, the time evolution operator $\mathcal{U} = \mathcal{T}\exp[-i\int_{t_i}^{t_f} dt\, H(t)]$ is determined by the Hamiltonian $H(t) = H_{\rm sys} + H_{\Gamma_f} + H_\Gamma(t)$, where $\mathcal{T}$ is the time-ordering operator and the interaction part $H_\Gamma(t) = e^{iH_{\rm w}t}H_\Gamma e^{-iH_{\rm w}t}$ is

$$H_\Gamma(t) = \sum_k (r_k^\dagger O_{k,+}e^{ikt} + l_k^\dagger O_{k,-}e^{-ikt}) + {\rm H.c.} \quad (16)$$

In terms of $\mathcal{U}$, the amplitude (15) reads

$$\mathcal{A}_J(T) = {}_{\rm sys}\langle\varphi_{\rm out}|_{\rm b}\langle\{J_{k\alpha,\rm out}\}|\mathcal{U}|\{J_{k\alpha,\rm in}\}\rangle_{\rm b}|\varphi_{\rm in}\rangle_{\rm sys}, \quad (17)$$

where $J_{k\alpha,\rm in} = J_{k\alpha}e^{i\varepsilon_{k\alpha}t_i}$, $J_{k\alpha,\rm out} = J_{k\alpha}e^{i\varepsilon_{k\alpha}t_f}$, the dispersion relations $\varepsilon_{k,\alpha} = \sigma_\alpha k$, and $\sigma_{r(l)} = \pm$ for the right- and left-moving modes, respectively.

The displacement transformation U: $|\{J_{k\alpha}\}\rangle = e^{\sum_{k\alpha} |J_{k\alpha}|^2/2}U|\{0_{k\alpha}\}\rangle$ is introduced to rewrite the amplitude

$$\mathcal{A}_J(T) = \exp\left(\sum_{k,\alpha=r,l} |J_{k,\alpha}|^2 e^{-i\varepsilon_{k,\alpha}T}\right)$$

$$\times {}_{\rm sys}\langle\varphi_{\rm out}|_{\rm b}\langle\{0_{k\alpha}\}|\tilde{U}|\{0_{k\alpha}\}\rangle_{\rm b}|\varphi_{\rm in}\rangle_{\rm sys}, \quad (18)$$

where the state of the waveguide photon is transformed to the vacuum state, and the time evolution operator $\tilde{U} = \mathcal{T}e^{-i\int_{t_i}^{t_f} dt[H(t)+H_d(t)]}$ is determined by $H(t)$ and the driving term

$$H_d(t) = \sum_{k,\alpha=r,l} \left[J_{k,\alpha}^* O_{k,\sigma_\alpha} e^{-i\sigma_\alpha k(t_f-t)} + J_{k,\alpha} O_{k,\sigma_\alpha}^\dagger e^{-i\sigma_\alpha k(t-t_i)} \right]. \tag{19}$$

It follows from Eq. (14) that the functional derivative of $\mathcal{A}_J(T)$ determines the transition amplitude $\mathcal{A}(T)$, which is composed of Fourier transforms of time ordered correlators

$$\mathcal{G}(T) = \langle \mathcal{T} \gamma_{\text{out}}(t_f) O_1(t_1) \cdots O_n(t_n) \gamma_{\text{in}}^\dagger(t_i) \rangle \tag{20}$$

on the ground state $|\{0_k\}\rangle_b |G\rangle_{\text{sys}}$. Here, $O_j(t_j) = \mathcal{U}^\dagger(t) O_j \mathcal{U}(t)$ is given by the emitter operators $O_j = O_{k_j,\pm}$ and $O_{k_j,\pm}^\dagger$.

By the quantum regression theorem, as shown in Ref. [42], the bath degree of freedom can be traced out and the correlator

$$\mathcal{G}(T) = {}_{\text{sys}}\langle G|\mathcal{T} \gamma_{\text{out}}(t_f) O_{\text{eff},1}(t_1) \cdots O_{\text{eff},n}(t_n) \gamma_{\text{in}}^\dagger(t_i)|G\rangle_{\text{sys}}$$

becomes the average value of emitter operators $O_{\text{eff},j}(t) = \mathcal{U}_{\text{eff}}^\dagger(t) O_j \mathcal{U}_{\text{eff}}(t)$ on the ground state $|G\rangle_{\text{sys}}$. The time-evolution operator $\mathcal{U}_{\text{eff}}(t) = \exp(-i H_{\text{eff}} t)$ is given by the non-Hermitian effective Hamiltonian $H_{\text{eff}} = H_{\text{sys}} + H_{\text{decay}}$, where

$$H_{\text{decay}} = -i \sum_i \Gamma_{f,i} \tilde{O}_i^\dagger \tilde{O}_i - i \sum_{ij} \sqrt{\Gamma_i \Gamma_j} O_i^\dagger O_j e^{ik_0|x_i-x_j|}, \tag{21}$$

and $\Gamma_{f,i}$ is the decay rate to the free space of the emitter at the position x_i.

Based on the quantum regression theorem, each term in $\mathcal{A}(T)$ is related to the correlator of emitter operators $O_{\text{eff},j}(t)$ governed by the effective Hamiltonian H_{eff}. The resummation of these terms results in $\mathcal{A}(T) = \mathcal{F}_{\text{out}}^* \mathcal{F}_{\text{in}} \mathcal{A}_J(T)$ with the compact form

$$\mathcal{A}_J(T) = {}_{\text{sys}}\langle \varphi_{\text{out}}|\mathcal{U}_{\text{eff}}|\varphi_{\text{in}}\rangle_{\text{sys}} e^{\sum_{k,\alpha=r,l} |J_{k,\alpha}|^2 e^{-i\varepsilon_{k,\alpha}T}}, \tag{22}$$

where $\mathcal{U}_{\text{eff}} = \mathcal{T}e^{-i\int_{t_i}^{t_f} dt(H_{\text{eff}}+H_d)}$. Equations (14) and (22) establish the relation between the transition amplitude $\mathcal{A}(T)$ and the time-ordered correlators of emitters governed by the effective Hamiltonian H_{eff}.

By different choices of γ_{in}, γ_{out}, t_i, t_f, $\mathcal{F}_{\text{in}}$, and $\mathcal{F}_{\text{out}}$, the dynamics of the global system can be fully characterized. Hereafter, we refer the choice of $\gamma_{\text{in(out)}}$, $t_{(i,f)}$, and $\mathcal{F}_{\text{in(out)}}$ as the boundary condition. For instance, $\mathcal{A}(T)$ with the boundary condition $\gamma_{\text{in}} = \gamma_{\text{out}} = I$ (identity operator), $t_i \to -\infty$, and $t_f \to \infty$ leads to the photonic S matrix. For the boundary condition $\gamma_{\text{in}} = I$, $\gamma_{\text{out}} \neq I$, $t_i = 0$, and $t_f = T$, $\mathcal{A}(T)$ describes how the incident photons transform to the emitter excitations and propagate in the transient regime. For the boundary conditions $\gamma_{\text{in}} \neq I$, $\gamma_{\text{out}} = I$, $t_i = 0$, and $t_f = T$, the behaviors of spontaneous and stimulated emissions can be investigated by $\mathcal{A}(T)$. Using Eqs. (14), (21), and (22), together with different boundary conditions, we shall study the few-photon scattering process in the five models in Secs. IV–VII.

B. Generalized master equation

In order to study the dynamics of emitters during the scattering, one can either use the transition amplitude (14) with proper boundary conditions or derive the master equation of emitter reduced density operator by tracing out the photonic degree of freedom. In quantum optics, the initial states of the photonic bath are usually the vacuum state, the thermal state, and Gaussian states, where the conventional master equation is obtained based on the Born-Markov approximation.

During the scattering process, the initial state of photons is dramatically changed. For instance, the single incident photon resonant with the transition energy of the two-level emitter is totally reflected, as predicted by the single-photon scattering theory [3,12,21,22], where the photon in the initial asymptotic state $r_k^\dagger|0\rangle$ is totally scattered to the photon in the outgoing asymptotic state $l_{-k}^\dagger|0\rangle$. However, the conventional master equation assumes that the initial state of the photonic bath is unchanged, and the state of the global system is always the product state of the emitter and the photonic bath [18]. This assumption contradicts the exact result of the single-photon scattering theory, thus, the conventional master equation breaks down. The generalized master equation is required to investigate the dynamics of emitters in the few-photon scattering process.

For the initial state of few photons in the waveguide, the evolution of the system state is described by the reduced density matrix $\rho_s(T) = Tr_{\text{bath}}[\mathcal{U}\rho(0)\mathcal{U}^\dagger]$, where in terms of the coherent state $|\{J_{k\alpha}\}\rangle$

$$\rho(0) = \mathcal{F}_{\text{in}}^* \mathcal{F}_{\text{in}}[\rho_{\text{sys}}(0) \otimes |\{J_{k\alpha}\}\rangle_b \langle\{J_{k\alpha}\}|]. \tag{23}$$

The displacement transformation U relates the density matrix

$$\rho_s(T) = \mathcal{F}_{\text{in}}^* \mathcal{F}_{\text{in}} e^{\sum_{k\alpha} |J_{k\alpha}|^2} \rho_J(T) \tag{24}$$

to the generating density matrix

$$\rho_J(T) = Tr_{\text{bath}}[\mathcal{U}_J \rho_{\text{sys}}(0) \otimes |\{0_{k\alpha}\}\rangle\langle\{0_{k\alpha}\}|\mathcal{U}_J^\dagger], \tag{25}$$

where $\mathcal{U}_J = U^\dagger \mathcal{U} U$ describes the evolution of emitters under the driving field. In $\rho_J(T)$, the initial state of photons is transformed to the vacuum state, thus, the conventional master equation can be used to describe the time evolution of $\rho_J(T)$. Under the Markov approximation, the master equation governing the evolution of $\rho_J(T)$ reads

$$\partial_T \rho_J(T) = -i[\tilde{H}_{\text{sys}}, \rho_J(T)] + \mathcal{L}\rho_J(T), \tag{26}$$

where the initial condition is $\rho_J(0) = \rho_{\text{sys}}(0)$. The displacement transformation induces the driving term in

$$\tilde{H}_{\text{sys}} = H_{\text{sys}} + \sum_{ij} \sqrt{\Gamma_i \Gamma_j} O_i^\dagger O_j \sin(k_0|x_i - x_j|)$$
$$+ \sum_{k,\alpha} \left(J_{k,\alpha}^* O_{k,\sigma_\alpha} e^{i\sigma_\alpha kT} + J_{k,\alpha} O_{k,\sigma_\alpha}^\dagger e^{-i\sigma_\alpha kT} \right), \tag{27}$$

and the Lindblad operator is

$$
\mathcal{L}\rho_J(T) = 2\sum_{ij} \sqrt{\Gamma_i \Gamma_j} O_i \rho_J(T) O_j^\dagger \cos[k_0(x_i - x_j)]
$$
$$
- \sum_{ij} \sqrt{\Gamma_i \Gamma_j} \cos[k_0(x_i - x_j)]\{O_i^\dagger O_j, \rho_J(T)\}
$$
$$
+ \sum_i \Gamma_{f,i}[2\tilde{O}_i \rho_J(T)\tilde{O}_i^\dagger - \{\tilde{O}_i^\dagger \tilde{O}_i, \rho_J(T)\}].
$$
$$(28)$$

The generalized master equations (24) and (26) are the main results in this section, which lead to some significant results: (a) In principle, once $\rho_J(T)$ is obtained, $\rho_s(T)$ is determined through Eq. (24), which describes the transient dynamics of emitters during the scattering processes. In practice, the evolution of emitters for the few incident photons can be studied by the perturbative expansion of the classical sources $J_{k,\alpha}$ and $J_{k,\alpha}^*$. For instance, for the single incident photon, Eq. (24) contains at most the second order derivative $\delta^2 \rho_J(T)/\delta J_{p\alpha'}^* \delta J_{k\alpha}$; the second order perturbative expansion of $J_{k,\alpha}$ and $J_{k,\alpha}^*$ in $\rho_J(T)$ determines $\rho_s(T)$. Here, the zero order and second order contributions lead to the emitter reduced density matrix for the single incident photon. The zero order contribution $\rho_{\text{sys}}(0)$ describes the unchanged emitter state without interacting with the photon, while the second order contribution $\mathcal{F}_{\text{in}}^* \mathcal{F}_{\text{in}} \rho_J(T)$ describes the dynamics of emitters responding to the single incident photon. Similarly, for two incident photons, the reduced density matrix can be determined by the fourth order expansion of $J_{k,\alpha}$ and $J_{k,\alpha}^*$.

(b) In quantum optics, we are interested in the transmission properties of weak probe light to emitters, i.e., the transmission spectrum and the quantum statistics. We notice that Eq. (26) just describes the emitters under the classical probe light with the strength $J_{k\alpha}$. If the driving field is weak, we can solve Eq. (26) by the perturbative expansion of $J_{k,\alpha}$ and $J_{k,\alpha}^*$. As we discussed above, the second and fourth order perturbative expansions describe the transient dynamics of emitters in the single- and two-photon scattering processes. As a result, the quantum properties of outgoing photons and emitters under the weak driving light can be studied by the few-photon scattering theory, where only the time evolution in the forward path is involved, as shown in Eq. (22). We shall show in Sec. VII that for the emitters with complicated structures the scattering theory is still able to provide the analytic results, which perfectly agree with the numerical results from the master equation approach. The few-photon scattering theory enables us to analytically investigate the quantum properties of photons from emitters under the weak driving field.

(c) If we set the external source to be zero, Eq. (26) agrees with the master equation [32] for the photonic bath initially in the ground state.

C. Exact S matrix by path integral approach

Equations (14), (21), and (22) in Sec. III A relate the transition amplitude to the correlators of emitters governed by the effective Hamiltonian, where under the Markov approximation the quantum regression theorem leads to the instantaneous effective Hamiltonian. In this section, we show the exact result of the transition amplitude (14), from which the result obtained

by the quantum regression theorem is proven to be exact for the single emitter coupled to the waveguide. The validity of the Markov approximation and some non-Markov effects for several emitters coupled to the waveguide will be investigated by the exact transition amplitude in Sec. VI.

Following the procedure of path integral formalism, we discretize the evolution time T by $N \to \infty$ instants $\{t_1 \cdots t_N\}$ and insert a coherent state basis at each instant t_i. By integrating out the free space modes we obtain

$$
\mathcal{A}_J(T) = \int D[\text{system}]\gamma_{\text{out}}(t_f)\gamma_{\text{in}}^*(t_i)e^{iS_{\text{sys}}}
$$
$$
\times \int D[\alpha_k, \alpha_k^*]e^{\sum_{k,\alpha} J_{k,\alpha}^* \alpha_k(t_f)} e^{iS}, \quad (29)
$$

where the action

$$
S = \int_{t_i}^{t_f} dt \left\{ \sum_k [r_k^*(i\partial_t - k)r_k + l_k^*(i\partial_t + k)l_k] - H_\Gamma \right\}
$$
$$(30)$$

describes free propagation of the right- and left-moving photons in the waveguide and the interaction with the emitters, and $\int D[\text{system}]$ is the integral over the emitter field. The action of the emitter is

$$
S_{\text{sys}} = S_{\text{sys}}^{(0)} + i \int_{t_i}^{t_f} dt \sum_i \Gamma_{f,i} \tilde{O}_i^\dagger \tilde{O}_i, \quad (31)
$$

where the first term is the action of emitters, and the second term describes the decay to the free space.

By $\delta S/\delta r_k^* = 0$ and $\delta S/\delta l_k^* = 0$, the classical motion equations read

$$
(i\partial_t - k)r_{k,\text{cl}} - O_{k,+} = 0,
$$
$$
(i\partial_t + k)l_{k,\text{cl}} - O_{k,-} = 0, \quad (32)
$$

which give the classical paths

$$
r_{k,\text{cl}}(t) = J_{k,r} e^{-ik(t-t_i)} - i \int_{t_i}^t ds\, O_{k,+}(s)e^{-ik(t-s)},
$$
$$(33)$$
$$
l_{k,\text{cl}}(t) = J_{k,l} e^{ik(t-t_i)} - i \int_{t_i}^t ds\, O_{k,-}(s)e^{ik(t-s)}.
$$

Following the saddle-point method, we expand the photon fields $r_k = r_{k,\text{cl}} + \delta r_k$ and $l_k = l_{k,\text{cl}} + \delta l_k$ by the quantum fluctuation fields δr_k and δl_k around the classical paths, and integrate out the fluctuation fields in $\mathcal{A}_J(T)$. Due to the quadratic form of the action (30),

$$
\mathcal{A}_J(T) = \exp\left(\sum_{k,\alpha} |J_{k,\alpha}|^2 e^{-i\sigma_\alpha kT}\right)
$$
$$
\times \int D[\text{system}]\gamma_{\text{out}}(t_f)\gamma_{\text{in}}^*(t_i)e^{iS_{\text{eff}} + iS_J} \quad (34)
$$

is obtained exactly, where the nonlocal effective action $S_{\text{eff}} = S_{\text{sys}} + S_{\text{re}}$ of emitters is determined by

$$
S_{\text{re}} = i \int_{t_i}^{t_f} dt \int_{t_i}^t ds \sum_k [O_{k,+}^*(t)O_{k,+}(s)e^{-ik(t-s)}
$$
$$
+ O_{k,-}^*(t)O_{k,-}(s)e^{ik(t-s)}], \quad (35)
$$

and the source terms $S_J = -\int_{t_i}^{t_f} dt\, H_{\text{d}}(t)$.

Equations (34) and (35) are the central results in this section. It follows from Eq. (14) that the functional derivatives of $\mathcal{A}_J(T)$ lead to the transition amplitude $\mathcal{A}(T)$. We also notice that, apart from the phase factor, $\mathcal{A}_J(T)$ is the generating functional [58] of the emitter correlators, namely, the functional derivatives of $\mathcal{A}_J(T)$ give the correlation functions of emitter operators. As a result, the transition amplitude $\mathcal{A}(T)$ is determined by the correlation functions of emitter fields, where the effective action S_{eff} is generally time nonlocal.

For the single emitter coupled to the waveguide with the linear dispersion, the action S_{eff} turns out to be time local, and the effective Hamiltonian H_{eff} is deduced. Here, the renormalized part (35) has the time-local form

$$S_{\mathrm{re}} = i\Gamma \int_{t_i}^{t_f} dt\, O^*(t)O(t),\tag{36}$$

and effective Hamiltonian

$$H_{\mathrm{eff}} = H_{\mathrm{sys}} - i\Gamma_f \tilde{O}^\dagger \tilde{O} - i\Gamma O^\dagger O\tag{37}$$

of emitters is obtained. In fact, the functional integral in Eq. (34) is just the amplitude $_{\mathrm{sys}}\langle\varphi_{\mathrm{out}}|\mathcal{U}_{\mathrm{eff}}|\varphi_{\mathrm{in}}\rangle_{\mathrm{sys}}$ in Eq. (22), thus, the result based on the quantum regression theorem agrees with the exact result (34).

For several emitters, the renormalization part

$$S_{\mathrm{re}} = i \int_{t_i}^{t_f} dt \sum_{ij} \sqrt{\Gamma_i\Gamma_j}\, O_i^*(t) O_j(t - |x_i - x_j|)e^{ik_0|x_i-x_j|}$$

is time nonlocal. If the wavelength of frequency fluctuations around k_0 is much larger than the size Nd of the emitter array, the time delay effect can be neglected, which leads to the time-local action

$$S_{\mathrm{re}} = i \int_{t_i}^{t_f} dt \sum_{ij} \sqrt{\Gamma_i\Gamma_j}\, O_i^*(t) O_j(t)e^{ik_0|x_i-x_j|},\tag{38}$$

and the effective Hamiltonian (21). In this limit, the result (22) agrees with the exact result (34) for several emitters.

At the end of this section, we briefly summarize the results. We use two approaches to obtain the transition amplitude and the generalized master equation for the photon scattering process, where the derivation of the generalized master equation (26) from the path integral approach is left in the Appendix. The relation between the few-photon scattering by emitters and the emitters under weak driving light is established. For the single emitter case, the result (22) based on the quantum regression theorem is proven to be exact. For several emitters, in the Markovian limit, the result (22) agrees with the exact result from the path integral approach.

IV. PARADIGMATIC EXAMPLES

In this section, as paradigmatic examples, the few-photon scattering by the single emitter is studied by the scattering theory developed in Sec. III. The emitter is chosen to be the two-level emitter or the JC system, where the decay to the free space is neglected, i.e., $\Gamma_f = 0$. For the two-level emitter, we investigate the transmission spectra and the quantum statistics of outgoing photons for the single and two incident photons. For the emitter initially in the excited state without the incident photon, the spontaneous emission of the emitter is studied. The

transient process, i.e., the response of the two-level emitter in the ground state to the single-photon wave packet, is analyzed by the exact transition amplitude of the emitter in the excited state. For the stimulated emission of the two-level emitter initially in the excited state, the wave-packet shape of the single incident photon is designed, such that the probability of stimulated emission is maximal. For the JC system, we show the transmission spectra and the quantum statistics of scattering photons. By these two examples, we examine our theory by a comparison with the well-known results in Refs. [21–23,53], which justifies the correctness of the developed scattering theory.

A. Two-level emitter

For the two-level emitter, $O = \sigma^-$ and the effective Hamiltonian $H_{\mathrm{eff}} = H_{\mathrm{sys}} - i\Gamma\sigma^+\sigma^-$ follows from Eq. (37), where H_{sys} vanishes in the rotating frame since the transition frequency $\omega_e = k_0$ is resonant with the central frequency of the waveguide. It follows from Eq. (19) that the external source term is

$$S_J = -\sqrt{\frac{\Gamma}{L}} \int_{t_i}^{t_f} dt \sum_{k,\alpha=r,l} [J_{k,\alpha}^* \sigma^-(t)e^{-i\sigma_\alpha k(t_f-t)}$$
$$+ J_{k,\alpha}\sigma^+(t)e^{-i\sigma_\alpha k(t-t_i)}].\tag{39}$$

For the scattering of single right-moving photon with the momentum k by the emitter in the ground state, the boundary condition in the asymptotic limit $t_i \to -\infty$ is $\gamma_{\mathrm{in}} = I$ and $\mathcal{F}_{\mathrm{in}} = \lim_{\{J_k\}\to 0} \delta/\delta J_{k,r}$. By the boundary condition $\gamma_{\mathrm{out}} = I$ and $\mathcal{F}_{\mathrm{out}} = \lim_{\{J_k\}\to 0} \delta/\delta J_{p,(r,l)}$ in the asymptotic limit $t_f \to \infty$, Eqs. (14) and (34) lead to the reflection and transmission coefficients

$$R_k\delta_{p,-k} = \frac{-i\Gamma}{k_0 + i\Gamma}\delta_{p,-k}\tag{40}$$

and

$$T_k\delta_{p,k} = \frac{k_0}{k_0 + i\Gamma}\delta_{p,k},\tag{41}$$

in the asymptotic limits $t_i \to -\infty$ and $t_f \to \infty$. For the scattering of two right-moving photons with momenta k_1 and k_2 by the emitter in the ground state, the boundary condition in the asymptotic limit $t_i \to -\infty$ is $\gamma_{\mathrm{in}} = I$ and $\mathcal{F}_{\mathrm{in}} = \lim_{\{J_k\}\to 0} \delta^2/\delta J_{k_1,r}\delta J_{k_2,r}$. By the boundary condition $\gamma_{\mathrm{out}} = I$ and $\mathcal{F}_{\mathrm{out}} = \lim_{\{J_k\}\to 0} \delta^2/\delta J_{-p_1,l}\delta J_{-p_2,l}$ in the asymptotic limit $t_f \to \infty$, it follows from Eqs. (14) and (34) that the S matrix

$$S_{p_1p_2;k_1k_2} = \Gamma^2 \int_{-\infty}^{+\infty} \frac{dt_1'dt_2'dt_1dt_2}{(2\pi)^2} e^{ip_1t_1'+ip_2t_2'-ik_1t_1-ik_2t_2}$$
$$\times \langle \mathcal{T}\sigma^-(t_1')\sigma^-(t_2')\sigma^+(t_1)\sigma^+(t_2)\rangle\tag{42}$$

of two reflected photons with momenta $-p_1$ and $-p_2$ is given by the time-ordered correlator of spin operators. Here, the time evolution $\sigma^\pm(t) = \sigma^\pm e^{\pm\Gamma t}$ governed by H_{eff} determines the four-point correlator, which leads to the S matrix

$$S_{p_1p_2;k_1k_2} = R_{k_1}R_{k_2}\big(\delta_{p_1k_1}\delta_{p_2k_2} + \delta_{p_1k_2}\delta_{p_2k_1}\big)$$
$$+ \frac{i\Gamma^2}{\pi}\frac{\delta_{p_1+p_2,k_1+k_2}(k_1+k_2+2i\Gamma)}{(p_1+i\Gamma)(p_2+i\Gamma)(k_1+i\Gamma)(k_2+i\Gamma)}.\tag{43}$$

The wave function of two reflected photons is obtained directly from the Fourier transform of Eq. (43) [22] as

$$\psi(x_1,x_2) = \frac{1}{2}\int dp_1 dp_2 e^{ip_1 x_1 + ip_2 x_2} S_{p_1 p_2; k_1 k_2}$$

$$= e^{iEx_c} R_{k_1} R_{k_2}[\cos(kx) - e^{[i(1/2)E - \Gamma]|x|}], \quad (44)$$

where the total momentum $E = k_1 + k_2$, the relative momentum $k = (k_1 - k_2)/2$, the center-of-mass coordinate $x_c = (x_1 + x_2)/2$, and the relative momentum $x = x_1 - x_2$. The results (43) and (44) agree with those in Refs. [21,22].

For two photons with the resonant frequency $k_1 = k_2 = 0$, the reflection coefficients are $R_{k_1} = R_{k_2} = 1$ and the wave function

$$\psi(x_c, x) = 1 - e^{-\Gamma|x|}. \quad (45)$$

In Sec. III, we prove that the quantum statistics of outgoing photons from the emitter under the weak driving light can be characterized by the two-photon wave function $\psi(x_c, x)$. More precisely, for the weak driving light with the zero detuning $\Delta_d = \omega_d - \omega_e$, the second order correlation function $g^{(2)}(x) = |\psi(x_c, x)|^2$ of the emitted photons can be obtained by the two-photon wave function $\psi(x_c, x)$ from the scattering theory. Here, $g^{(2)}(x) = (1 - e^{-\Gamma|x|})^2$ display the antibunching behavior.

The spontaneous decay of the two-level emitter in the excited state can be investigated by the boundary conditions $\gamma_{\rm in} = \sigma^-$, $\mathcal{F}_{\rm in} = 1$ and $\gamma_{\rm out} = I$, $\mathcal{F}_{\rm out} = \lim_{\{J_k\} \to 0} \delta/\delta J_{p,(r,l)}$ at the initial and the final instants $t_i = 0$ and $t_f = T$. Equations (14) and (34) give the amplitude

$$\mathcal{A}(T) = \sqrt{\frac{\Gamma}{2\pi}} \frac{e^{-i\sigma_\alpha pT} - e^{-\Gamma T}}{\sigma_\alpha p + i\Gamma} \quad (46)$$

to detect a single outgoing photon with the momentum p. The Fourier transform gives the wave function

$$\psi(x) = \int \frac{dp}{\sqrt{2\pi}} e^{ipx} \mathcal{A}(T)$$

$$= -i\sqrt{\Gamma} e^{-\Gamma(T - \sigma_a x)} \theta(T - \sigma_a x)\theta(\sigma_a x) \quad (47)$$

in the coordinate space for the right- and left-moving photons. Since the emitter couples to the left- and right-moving modes symmetrically, the wave packets of the right- and left-moving photons are symmetric with respect to the origin. As shown in Fig. 2(a), $|\psi(x)|^2$ for the right-moving photon exhibits the Lorentzian shape with the different widths $1/\Gamma$.

The reverse process of the spontaneous decay is the response of the two-level emitter in the ground state to the single-photon wave packet $f_{\rm in}(k)$. Here, the boundary conditions are $\gamma_{\rm in} = I$, $\mathcal{F}_{\rm in} = \lim_{\{J_k\} \to 0}\int dk f_{\rm in}(k)\delta/\delta J_{k,r}$ and $\gamma_{\rm out} = \sigma^-$ and $\mathcal{F}_{\rm out} = 1$ at the instants $t_i = 0$ and $t_f = T$, respectively. Equations (14) and (34) result in the amplitude

$$\mathcal{A}(T) = -i\sqrt{\frac{\Gamma}{2\pi}}\int dk f_{\rm in}(k)\int_0^T dt\, e^{-ikt}\langle\sigma^-(T)\sigma^+(t)\rangle$$

$$= \sqrt{\frac{\Gamma}{2\pi}}\int dk f_{\rm in}(k)\frac{e^{-ikT} - e^{-\Gamma T}}{k + i\Gamma} \quad (48)$$
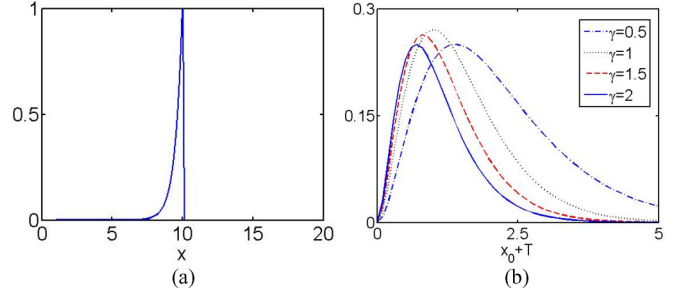
FIG. 2. (Color online) Emission and absorption of a single photon by a single emitter: (a) The spatial amplitude $|\psi(x)|^2$ of a right-propagating single-photon wave packet, produced by an emitter initially prepared in the excited state at $T = 0$. The wave packet shown here is after an evolution time $T = 10/\Gamma$. (b) The probability $|A(T)|^2$ of the emitter in the excited state for the incident wave packet with the width $1/\gamma$ and localized at x_0. Here, the emission rate $\Gamma = 1$ into the waveguide is taken to be the unit.

of the emitter in the excited state. For the right-moving photon wave packet

$$f_{\rm in}(k) = \sqrt{\frac{\gamma}{\pi}}\frac{e^{-ikx_0}}{k + i\gamma} \quad (49)$$

with the width $1/\gamma$ initially at the position $x_0 < 0$, the residue theorem gives

$$\mathcal{A}(T) = \frac{\sqrt{2\gamma\Gamma}}{\Gamma - \gamma}[e^{-\Gamma(x_0 + T)} - e^{-\gamma(x_0 + T)}]\theta(x_0 + T). \quad (50)$$

In Fig. 2(b), we show $|\mathcal{A}(T)|^2$ of the emitter in the excited state for different widths γ.

In the stimulated emission, the two-level emitter is initially prepared in the excited state at the instant $t_i = 0$, and the wave packet of single right-moving photon is designed to realize the maximal probability of emitting two right-moving photons in the asymptotic limit $t_f \to \infty$.

With the initial and final boundary conditions $\gamma_{\rm in} = \sigma^-$, $\mathcal{F}_{\rm in} = \lim_{\{J_k\}\to 0}\int dk\, f_{\rm in}(k)\delta/\delta J_{k,r}$ and $\gamma_{\rm out} = I$, $\mathcal{F}_{\rm out} = \lim_{\{J_k\}\to 0}\delta^2/\delta J_{p_1,r}\delta J_{p_2,r}$, Eqs. (14) and (34) result in the S matrix

$$S_{p_1 p_2,k} = \sqrt{\frac{\Gamma}{2\pi}}\int dk\, f_{\rm in}(k)\left[\delta_{kp_1}\frac{1}{p_2 + i\Gamma} + \frac{\Gamma}{2\pi}\frac{1}{p_1 + i\Gamma}\right.$$

$$\left.\times \frac{1}{p_1 - k + i0^+}\frac{1}{p_1 + p_2 - k + i\Gamma}\right] + (p_1 \leftrightarrow p_2)$$

$$(51)$$

of two right-moving photons with momenta p_1 and p_2. The Fourier transform of $S_{p_1 p_2,k}$ results in the wave function

$$\psi(x_1,x_2) = \int \frac{dp_1 dp_2}{2\pi} S_{p_1 p_2,k} e^{ip_1 x_1 + ip_2 x_2}$$

$$= \int dx\, f_{\rm in}(x)[\mathcal{B}(x_1,x_2;x) + \mathcal{B}(x_2,x_1;x)], \quad (52)$$

in the coordinate space, where

$$\mathcal{B}(x_1,x_2;x) = -i\sqrt{\Gamma} e^{\Gamma x_2}\theta(-x_2)[\delta(x - x_1)$$

$$- \Gamma e^{-\Gamma(x - x_1)}\theta(x_2 - x)\theta(x - x_1)], \quad (53)$$

and

$$f_{\text{in}}(x) = \int \frac{dk}{\sqrt{2\pi}} f_{\text{in}}(k) e^{ikx} \tag{54}$$

describes the incident wave packet in the coordinate space.

We design the shape of the wave packet $f_{\text{in}}(x)$ to maximize the stimulated emission probability

$$P_{\text{st}} = \frac{1}{2} \int dx_1 dx_2 |\psi(x_1, x_2)|^2. \tag{55}$$

The amplitude (52) leads to

$$P_{\text{st}} = \int dx \, dy f_{\text{in}}^*(x) W(x, y) f_{\text{in}}(y), \tag{56}$$

where

$$W(x, y) = \int dx_1 dx_2 \mathcal{B}^*(x_1, x_2; x)$$
$$\times [\mathcal{B}(x_1, x_2; y) + \mathcal{B}(x_2, x_1; y)]. \tag{57}$$

The function (53) gives

$$W(x, y) = \frac{1}{2} \delta(y - x) + \frac{\Gamma}{4} (3e^{\Gamma(x+y)} - e^{-\Gamma|x-y|}) \theta(-x) \theta(-y).$$

The manifest effect of two photons to the system is realized by the initial wave packet $f_{\text{in}}(x)$ localized at $x < 0$. The largest eigenvalue of $W(x, y)$ gives the maximal probability of stimulated emission, and the corresponding eigenstate determines the shape of the single-photon wave function $f_{\text{in}}(x)$.

Fortunately, the eigenequation, i.e., the integral equation

$$\int_{-\infty}^{0} dy \, W(x, y) f_{\text{in}}(y) = \lambda f_{\text{in}}(x) \tag{58}$$

can be solved exactly. In Eq. (58), the second order derivative to x leads to the differential equation

$$\partial_x^2 f_{\text{in}}(x) = \frac{\lambda}{\lambda - \frac{1}{2}} \Gamma^2 f_{\text{in}}(x), \tag{59}$$

where the solution is

$$f_{\text{in}}(x) = \left(\frac{4\Gamma^2 \lambda}{\lambda - \frac{1}{2}} \right)^{1/4} \exp\left[\sqrt{\frac{\lambda}{\lambda - \frac{1}{2}}} \Gamma x \right] \theta(-x). \tag{60}$$

The eigenvalue $\lambda = 2/3$ is obtained by the fact that $f_{\text{in}}(x)$ is the solution of Eq. (58). Finally, we conclude that the largest probability of stimulated emission in the two-level emitter is $P_{\text{st}}^{\max} = 2/3$, and the corresponding incident wave packet is $f(x) = 2\sqrt{\Gamma} e^{2\Gamma x} \theta(-x)$.

We notice that this result agrees with that in Ref. [53], where two types of the incident wave packets, i.e., the Gaussian type and the Lorentzian shape are considered. By tuning the width of the wave packet, the maximal probability 2/3 of the stimulated emission was found for the initial wave packet with the Lorentzian shape. Here, we proved the exact result $P_{\text{st}}^{\max} = 2/3$ by solving the integral equation (58) analytically.

B. JC system

In this section, we consider the JC system as the single emitter coupled to waveguide photons, and apply the scattering theory to study the different scattering processes. The emitter Hamiltonian in the rotating frame reads

$$H_{\text{sys}} = \Delta_c a^\dagger a + \Delta_e |e\rangle\langle e| + g(a^\dagger |g\rangle\langle e| + \text{H.c.}), \tag{61}$$

where the detunings are $\Delta_c = \omega_c - k_0$ and $\Delta_e = \omega_e - k_0$. For convenience, we focus on the resonant case $\Delta_c = \Delta_e = 0$. The effective Hamiltonian $H_{\text{eff}} = H_{\text{sys}} - i\Gamma a^\dagger a$ follows from Eq. (37). The external source term is

$$S_J = -\sqrt{\frac{\Gamma}{L}} \int_{t_i}^{t_f} dt \sum_{k,\alpha=r,l} [J_{k,\alpha}^* a(t) e^{-i\sigma_\alpha k(t_f-t)}$$
$$+ J_{k,\alpha} a^\dagger(t) e^{-i\sigma_\alpha k(t-t_i)}]. \tag{62}$$

For the single incident photon with the momentum k and the emitter initially in the ground state, the boundary condition is $\gamma_{\text{in}} = I$ and $\mathcal{F}_{\text{in}} = \lim_{\{J_k\}\to 0} \delta/\delta J_{k,r}$ in the asymptotic limit $t_i \to -\infty$. By the boundary condition $\gamma_{\text{out}} = I$ and $\mathcal{F}_{\text{out}} = \lim_{\{J_k\}\to 0} \delta/\delta J_{p,(r,l)}$ in the asymptotic limit $t_f \to \infty$, Eqs. (14) and (34) lead to the reflection and transmission coefficients

$$R_k \delta_{p,-k} = -\frac{i\Gamma k}{(k + i\Gamma)k - g^2} \delta_{p,-k},$$
$$T_k \delta_{p,k} = \frac{k^2 - g^2}{(k + i\Gamma)k - g^2} \delta_{p,k}. \tag{63}$$

For the two incident photons with momenta k_1 and k_2 to the emitter initially in the ground state, the boundary condition is $\gamma_{\text{in}} = I$ and $\mathcal{F}_{\text{in}} = \lim_{\{J_k\}\to 0} \delta^2/\delta J_{k_1,r}\delta J_{k_2,r}$ in the asymptotic limit $t_i \to -\infty$. By the boundary condition $\gamma_{\text{out}} = I$ and $\lim_{\{J_k\}\to 0} \delta^2/\delta J_{-p_1,l}\delta J_{-p_2,l}$ in the asymptotic limit $t_f \to \infty$, Eqs. (14) and (34) lead to the S-matrix element

$$S_{p_1 p_2;k_1 k_2} = \Gamma^2 \int_{-\infty}^{+\infty} \frac{dt_1' dt_2' dt_1 dt_2}{(2\pi)^2} e^{ip_1 t_1' + ip_2 t_2' - ik_1 t_1 - ik_2 t_2}$$
$$\times \langle \mathcal{T} a(t_1') a(t_2') a^\dagger(t_1) a^\dagger(t_2) \rangle, \tag{64}$$

of two reflected photons with momenta $-p_1$ and $-p_2$. Here, the correlator for operators $a(t) = e^{iH_{\text{eff}}t} a e^{-iH_{\text{eff}}t}$ and $a^\dagger(t) = e^{iH_{\text{eff}}t} a^\dagger e^{-iH_{\text{eff}}t}$ leads to the S-matrix element

$$S_{-p_1 -p_2;k_1 k_2} = R_{k_1} R_{k_2} \left(\delta_{p_1 k_1} \delta_{k_2 p_2} + \delta_{p_2 k_1} \delta_{k_2 p_1} \right)$$
$$+ i\frac{\Gamma^2}{\pi} \frac{g^4(E + i\Gamma)\delta_{p_1+p_2,k_1+k_2}}{(E + i\Gamma)(E + 2i\Gamma) - 2g^2}$$
$$\times \frac{E(E + 2i\Gamma) - 4g^2}{\prod_{i=1,2}[k_i(k_i + i\Gamma) - g^2][p_i(p_i + i\Gamma) - g^2]}. \tag{65}$$

The Fourier transform of Eq. (65) leads to the wave function

$$\psi(x_c, x) = \frac{1}{2} \sum_{p_1 p_2} S_{p_1 p_2;k_1 k_2} e^{ip_1 x_1 + ip_2 x_2}$$

$$= e^{iE x_c} \left\{ R_{k_1} R_{k_2} \cos(kx) \right.$$

$$- \frac{\Gamma^2 g^4}{\lambda_+ - \lambda_-} \frac{\sum_{s=\pm} s(E - 2\lambda_s) e^{i[(E/2)-\lambda_{-s}]x}}{(E + i\Gamma)(E + 2i\Gamma) - 2g^2}$$

$$\times \left. \frac{1}{\prod_{i=1,2}[k_i(k_i + i\Gamma) - g^2]} \right\} \tag{66}$$

of two photons, where λ_s is the solution of $k^2 + i\Gamma k - g^2 = 0$. As we discussed in Sec. III, under the weak driving light with frequency ω_d, the quantum statistics of photons emitting from the JC system can be described by the second order correlation function $g^{(2)}(x) = |\psi(x_c, x)|^2$, where $\psi(x_c, x)$ is the two-photon wave function for the incident photons with frequency $k_1 = k_2 = \omega_d - k_0$. The above results agree with those in Ref. [23].

As a summary, in this section, we use the single emitter case as the example to show how our theory works in the few-photon scattering process. All the results agree with the previous studies, which justifies the validity of the developed scattering theory.

V. VALIDITY OF MARKOV APPROXIMATION

In this section, we use the simple example to study the condition of the Markov approximation in the array of two-level emitters. As shown in Secs. III and IV, the dynamics of the single emitter coupled to the waveguide with the linear dispersion can be exactly described by the effective Hamiltonian (37) and the generalized master equation (26). For the array of emitters, the dynamics is exactly characterized by the effective time-nonlocal action S_{eff}, where the effective Hamiltonian (37) and the generalized master equation (26) only describe the emitter evolution under the Markov approximation.

In order to justify the validity of Markov approximation, we compare the exact result given by the path integral approach and the approximate result based on the quantum regression theorem. This comparison shows that the exact result and Markovian limit coincide when the bandwidth of the dynamics is sufficiently small compared to the distance between emitters.

We focus on the single- and two-photon scattering processes, where the effective action

$$S_{\text{eff}} = \int d\omega \sum_{ij} b_i^\dagger(\omega)[\omega I - \mathcal{H}_0(\omega)]_{ij} b_j(\omega)$$
$$- \frac{U_0}{2} \int dt \sum_j b_j^\dagger(t) b_j^\dagger(t) b_j(t) b_j(t) \tag{67}$$

of emitters is given by the matrix with elements $[\mathcal{H}_0(\omega)]_{ij} = -i\Gamma_f \delta_{ij} - i\Gamma e^{i(k_0+\omega)|x_i-x_j|}$. The driving action $S_J = -\int_{t_i}^{t_f} dt\, H_d(t)$ is given by Eq. (19) with $O_{k,\sigma_\alpha} = \sqrt{\Gamma/L} \sum_j e^{-i(k+\sigma_\alpha k_0)x_j} b_j$. Equations (14) and (34) lead to the exact results of the transmission spectrum and the second order correlation function by the effective action S_{eff} and S_J. Under the Markov approximation, Eqs. (14) and (34) give approximate results by the effective Hamiltonian $\mathcal{H}_0(\omega) \sim \mathcal{H}_0(0) \equiv \mathcal{H}_0^{\text{M}}$ and $O_{k,\sigma_\alpha} \sim O_{0,\sigma_\alpha}$.

A. Single-photon processes

For the single incident photon with the momentum k and the emitters initially in the ground state, the boundary condition is $\gamma_{\text{in}} = I$ and $\mathcal{F}_{\text{in}} = \lim_{\{J_k\}\to 0} \delta/\delta J_{k,r}$ in the asymptotic limit $t_i \to -\infty$. It follows from Eqs. (14) and (34) that the reflection
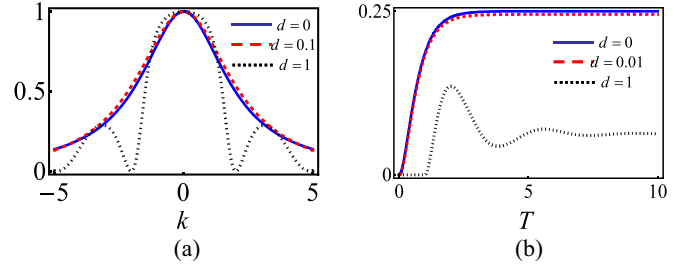
FIG. 3. (Color online) (a) Single incident photon reflection spectra in a two-emitter system, where the distance between emitters is d. (b) Excitation probability of second emitter $|A(2,T)|^2$ as a function of time T in a two-emitter system, when the second (first) emitter is initially prepared in the ground (excited) state. Here, $\Gamma_f = 0$ and Γ is taken as the unit. The Markovian results are also given by the solid (blue) curves.

coefficient

$$R_k = -i\Gamma \sum_{ij} [G(k)]_{ij} e^{i(k+k_0)(x_i+x_j)} \tag{68}$$

of the photon with momentum $p = -k$ is determined by the boundary condition $\gamma_{\text{out}} = I$ and $\mathcal{F}_{\text{out}} = \lim_{\{J_k\}\to 0} \delta/\delta J_{p,l}$ in the asymptotic limit $t_f \to \infty$, where the Green's function matrix $G(k) = [k - \mathcal{H}_0(k)]^{-1}$. In the Markovian limit, the reflection coefficient

$$R_k^{\text{M}} = -i\Gamma \sum_{ij} [G^{\text{M}}(k)]_{ij} e^{ik_0(x_i+x_j)}. \tag{69}$$

is determined by the approximate Green function $G^{\text{M}}(k) = [k - \mathcal{H}_0(0)]^{-1}$.

The difference in Eqs. (68) and (69) is that the phase factor e^{ikx_i} in $\mathcal{H}_0(k)$ is neglected in $G^{\text{M}}(k)$, which results in the condition $kNd \ll 1$ of the Markov approximation in the single-photon scattering. In Fig. 3(a), we show the reflection probabilities $|R_k|^2$ and $|R_k^{\text{M}}|^2$ of the scattering photon by two atoms with lattice spacing d, where $k_0 d = 2\pi n$ and n is an integer. The approximate result $|R_k^{\text{M}}|^2$ does not depend on d, which agrees with the exact result $|R_k|^2$ very well for small $kd \ll 1$. In the non-Markovian regime $kd > 1$, the dotted (black) curve ($d = 1$) shows that the reflection probability has the peaks localized around $n_0\pi/d$ and n_0 is an integer. The positions of these peaks are the resonant frequencies of eigenmodes in the "cavity" formed by the two emitters.

The behavior of single excitation propagation in the emitter array can also be analyzed by Eqs. (14) and (34), where the exact result gives the condition of the Markov approximation. For the first emitter initially in the excited state and the rest of the emitters in the ground state, the boundary conditions are $\mathcal{F}_{\text{in}} = I$ and $\gamma_{\text{in}} = b_1$ at the initial instant $t_i = 0$. The propagation of single excitation in the emitter array is described by the boundary condition $\mathcal{F}_{\text{out}} = I$ and $\gamma_{\text{out}} = b_j$ at the final instant $t_f = T$. Equations (14) and (34) lead to the amplitude

$$\mathcal{A}(j, T) = i \int \frac{d\omega}{2\pi} \left[\frac{1}{\omega - \mathcal{H}_0(\omega)} \right]_{j1} e^{-i\omega T} \tag{70}$$

of detecting the excitation at the jth emitter. The single photon emitted by the excitation of the first emitter is described by the amplitude

$$\mathcal{A}_\alpha(x,T) = -i\sqrt{\Gamma}\sum_j e^{-i\sigma_\alpha k_0 x_j}\theta[\sigma_\alpha(x-x_j)]$$
$$\times\,\theta[T-\sigma_\alpha(x-x_j)]\mathcal{A}(j,T-\sigma_\alpha(x-x_j)) \tag{71}$$

of detecting a single photon at the position x in the waveguide, where α denotes the right- and left-moving modes, and the boundary condition is $\mathcal{F}_{\text{out}}=\lim_{\{J_k\}\to 0}\delta/\delta J_{k,(r,l)}$ and $\gamma_{\text{out}}=I$ at the final instant $t_f=T$. In the Markovian limit, the amplitudes become

$$\mathcal{A}^{\text{M}}(j,T) = i\int\frac{d\omega}{2\pi}\left[\frac{1}{\omega-\mathcal{H}_0(0)}\right]_{j1}e^{-i\omega T} \tag{72}$$

and

$$\mathcal{A}^{\text{M}}_\alpha(x,T) = -i\sqrt{\Gamma}\sum_j e^{-i\sigma_\alpha k_0 x_j}\theta[\sigma_\alpha(x-x_j)]$$
$$\times\,\theta[T-\sigma_\alpha(x-x_j)]\mathcal{A}^{\text{M}}(j,T-\sigma_\alpha(x-x_j)). \tag{73}$$

To investigate the non-Markovian effects and justify the validity of the Markov approximation, we compare the exact results and the approximate results. It follows from the residue theorem that the poles ξ_λ and the corresponding residues Z_λ of $\{1/[\omega-\mathcal{H}_0(\omega)]\}_{j1}$ determine the time evolution $\mathcal{A}(j,T)\sim\sum_\lambda Z_\lambda e^{-i\xi_\lambda T}$. Similarly, $\mathcal{A}^{\text{M}}(j,T)\sim\sum_\lambda Z^{\text{M}}_\lambda e^{-i\xi^{\text{M}}_\lambda T}$ is given by the poles ξ^{M}_λ and the corresponding residues Z^{M}_λ of $\{1/[\omega-\mathcal{H}_0(0)]\}_{j1}$. Under the condition $\xi^{\text{M}}_\lambda Nd\ll 1$, the phase factor $e^{i\xi^{\text{M}}_\lambda|x_i-x_j|}\sim 1$, and ξ^{M}_λ and Z^{M}_λ are approximately the pole ξ_λ and the corresponding residue Z_λ of the exact propagator $\{1/[\omega-\mathcal{H}_0(\omega)]\}_{j1}$. As a result, the condition of the Markov approximation is $\xi^{\text{M}}_\lambda Nd\ll 1$.

To understand this condition, we consider two emitters in the waveguide, where the first emitter is placed at the origin, and the effective action is determined by the 2×2 matrix

$$\mathcal{H}_0(\omega) = \begin{pmatrix} -i\Gamma_f-i\Gamma & -i\Gamma e^{i(k_0+\omega)d} \\ -i\Gamma e^{i(k_0+\omega)d} & -i\Gamma_f-i\Gamma \end{pmatrix}. \tag{74}$$

It follows from Eqs. (70) and (71) that the exact amplitudes are

$$\mathcal{A}(1,T) = \tfrac{1}{2}e^{-(\Gamma_f+\Gamma)T}[C_+(T)+C_-(T)],$$
$$\mathcal{A}(2,T) = \tfrac{1}{2}e^{-(\Gamma_f+\Gamma)T}[C_-(T)-C_+(T)], \tag{75}$$

and

$$\mathcal{A}_\alpha(x,T) = -i\sqrt{\Gamma}\{\theta(\sigma_\alpha x)\theta(T-\sigma_\alpha x)\mathcal{A}(1,T-\sigma_\alpha x)$$
$$+\,e^{-i\sigma_\alpha k_0 d}\theta[\sigma_\alpha(x-d)]\theta[T-\sigma_\alpha(x-d)]$$
$$\times\,\mathcal{A}(2,T-\sigma_\alpha x+\sigma_\alpha d)\}, \tag{76}$$

where

$$C_\pm(T) = \sum_{n=0}^\infty\frac{1}{n!}[\pm\Gamma e^{ik_0 d+(\Gamma_f+\Gamma)d}(T-nd)]^n\theta(T-nd). \tag{77}$$

The amplitude $\mathcal{A}^{\text{M}}_\alpha(x,T)$ under the Markov approximation has the same form of Eq. (76), where $\mathcal{A}(j,T)$ is approximated by

$$\mathcal{A}^{\text{M}}(1,T) = \cosh(\Gamma T e^{ik_0 d})e^{-(\Gamma_f+\Gamma)T},$$
$$\mathcal{A}^{\text{M}}(2,T) = -\sinh(\Gamma T e^{ik_0 d})e^{-(\Gamma_f+\Gamma)T}. \tag{78}$$

The agreement between Eq. (78) and the exact result (75) is verified in the Markovian limit $(\Gamma_f+\Gamma)d\ll 1$, where $C_\pm(T)\sim e^{\pm\Gamma T e^{ik_0 d}}$.

The time evolution of the two emitters exhibits two non-Markovian effects. The first is the retardation effect. The amplitude $\mathcal{A}^{\text{M}}(2,T)$ shows that once $T>0$ the second emitter has the probability in the excited state. However, this is an artificial effect of the instantaneous effective Hamiltonian H_{eff} under the Markov approximation. In fact, the single-photon wave packet emitted by the first emitter takes the time $T=d$ to arrive at the second emitter. Hence, the second emitter has to stay at the ground state for $T<d$, i.e., $\mathcal{A}(2,T<d)=0$. This retardation effect is fully characterized by the exact result (75) and $C_\pm(T)$. We show the probability $|\mathcal{A}(2,T)|^2$ in Fig. 3(b) for $\Gamma_f=0$ and $k_0 d=2\pi n$, where the dotted (black) curve for $d=1$ displays the retardation effect explicitly. In the small d limit, i.e., $\Gamma d/c\ll 1$, the Markovian result agrees with the exact result very well, as shown by the solid (blue) and dashed (red) curves in Fig. 3(b), where the speed of light c is taken to be the unit.

The second effect is the formation of the entangle state $(|eg\rangle-|ge\rangle)/\sqrt{2}$ in the limit $T\to\infty$. For the vanishing $\Gamma_f=0$, both the exact and Markovian results show that in the steady state $T\to\infty$ the emitters have the probability P_e to form the entangle state. Under the Markov approximation, the probability $P_e=1/2$ is determined by $\mathcal{A}^{\text{M}}(1,\infty)=-\mathcal{A}^{\text{M}}(2,\infty)=1/2$. The exact result $\mathcal{A}(1,\infty)=-\mathcal{A}(2,\infty)=1/(2+2\Gamma d)$ gives the probability $P_e=1/[2(1+\Gamma d)^2]$ to form the entangle state. In the limit $\Gamma d\ll 1$, the Markov approximation works perfectly, i.e., $\mathcal{A}(j,\infty)\sim\mathcal{A}^{\text{M}}(j,\infty)=1/2$.

During the formation of the entangled state, the dynamics of the waveguide photon is described by the amplitudes $\mathcal{A}_{r,l}(x,T)$. In Fig. 4, we show the propagation of the right- and left-moving wave packets by $\mathcal{A}_{r,l}(x,T)$ for the distance $d=1$. In the steady state $T\to\infty$, the entangle state is established, where the standing wave in the regime $0<x<d$ forms to mediate the interaction of two emitters.

B. Two-photon processes

In this section, we study the scattering process of two incident photons with momenta k_1 and k_2. By comparing the exact result and the approximate result, we investigate the condition of the Markov approximation in the two-photon processes.

The initial boundary condition is $\gamma_{\text{in}}=I$ and $\mathcal{F}_{\text{in}}=\lim_{\{J_k\}\to 0}\delta^2/\delta J_{k_1,r}\delta J_{k_2,r}$ in the asymptotic limit $t_i\to-\infty$. It follows from Eqs. (14) and (34) that the S matrix

$$S_{p_1 p_2,k_1 k_2} = R_{k_1}R_{k_2}\big(\delta_{p_1 k_1}\delta_{p_2 k_2}+\delta_{p_2 k_1}\delta_{p_1 k_2}\big)$$
$$-\,i\frac{\Gamma^2}{\pi}\delta_{p_1+p_2,k_1+k_2}\sum_{ij}\bar{G}_i(p_1,p_2)T_{ij}(E)\bar{G}_j(k_1,k_2) \tag{79}$$
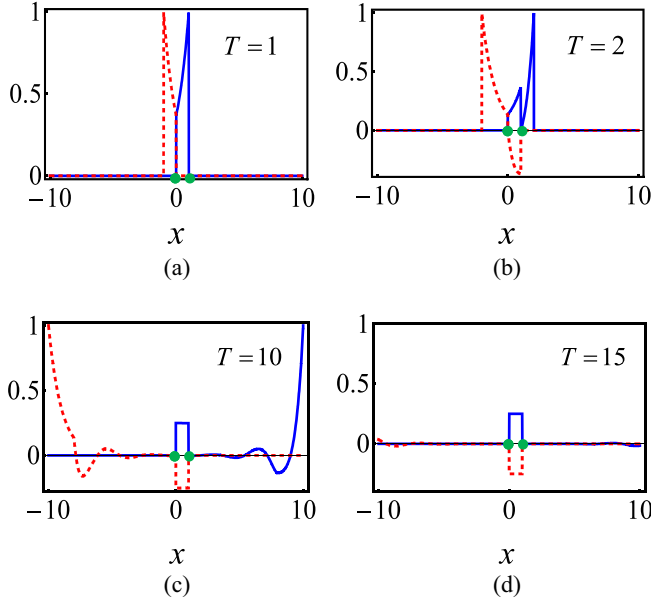
FIG. 4. (Color online) The solid (blue) and the dashed (red) curves show the wave functions of the right- and left-moving photons after the evolution time T, where the first (second) emitter is initially prepared in the excited (ground) state. Here, $\Gamma_f = 0$ and Γ is taken as the unit, and the green dots denote the two emitters.

of two reflected photons with momenta $-p_1$ and $-p_2$ are determined by the boundary condition $\gamma_{\text{out}} = I$ and $\mathcal{F}_{\text{out}} = \lim_{\{J_k\} \to 0} \delta^2/\delta J_{-p_1,l} \delta J_{-p_2,l}$ in the asymptotic limit $t_f \to \infty$. Here,

$$\bar{G}_i(p_1,p_2) = \sum_{i_1 i_2} G_{i_1 i}(p_1) G_{i_2 i}(p_2) e^{i(p_1+k_0)x_{i_1}} e^{i(p_2+k_0)x_{i_2}}, \tag{80}$$

and the T matrix $T(E) = -\Pi^{-1}(E)$ is given by the Dyson expansion with the bubble

$$\Pi_{ij}(E) = i \int \frac{d\omega}{2\pi} G_{ij}(\omega) G_{ij}(E-\omega) \tag{81}$$

and $E = k_1 + k_2$.

Under the Markov approximation, $S_{p_1 p_2, k_1 k_2}$ is given by the same form of Eq. (79), where $R_{k_i} \sim R_{k_i}^{\text{M}}$,

$$\bar{G}_i(p_1,p_2) \sim \sum_{i_1 i_2} G_{i_1 i}^{\text{M}}(p_1) G_{i_2 i}^{\text{M}}(p_2) e^{ik_0(x_{i_1}+x_{i_2})} \tag{82}$$

and the bubble (81) are determined by the approximate Green's function $G^{\text{M}}(\omega) \sim [\omega - \mathcal{H}_0(0)]^{-1}$. The exact result shows that the Markov approximation is valid in the limits $k_i N d$, $p_i N d$, and $\Gamma N d \ll 1$.

In order to understand the condition, we investigate the two-photon scattering processes explicitly by considering the photon scattering by two emitters, where $k_0 d = 2\pi n$. We first compare the exact T matrix $T(E)$ with the T matrix $T^{\text{M}}(E)$ under the Markov approximation, where the elements $\Pi_{11}^{\text{M}}(E) = \Pi_{22}^{\text{M}}(E) = \Pi_a^{\text{M}}(E) + \Pi_b^{\text{M}}(E)$ and $\Pi_{12}^{\text{M}}(E) =$
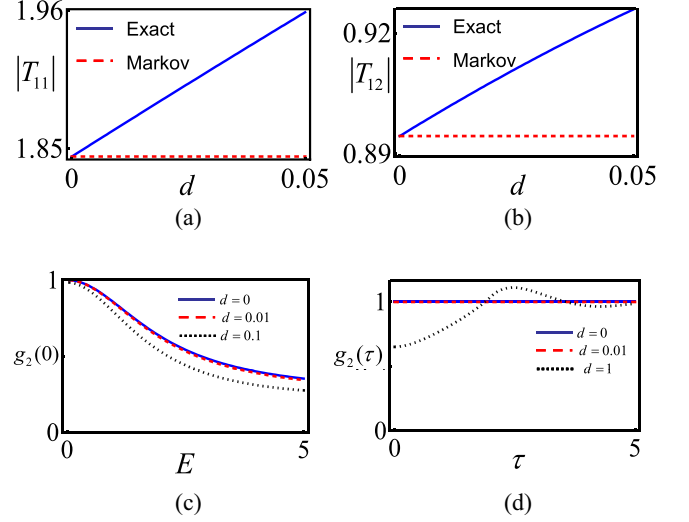
FIG. 5. (Color online) (a),(b) The exact and Markovian T-matrix elements for $E = 1$. (c),(d) The second order correlation functions of outgoing photons: In (c) $\tau = 0$, in (d) $E = 0$, and Markovian results are shown by the solid (blue) curves. Here, $\Gamma_f = 0$ and Γ is taken as the unit.

$\Pi_{21}^{\text{M}}(E) = \Pi_a^{\text{M}}(E) - \Pi_b^{\text{M}}(E)$ are given by

$$\Pi_a^{\text{M}}(E) = \frac{1}{4} \sum_{\sigma=\pm 1} \frac{1}{E + 2i\Gamma_f + 2i\Gamma(1 + \sigma e^{ik_0 d})},$$

$$\Pi_b^{\text{M}}(E) = \frac{1}{2} \frac{1}{E + 2i\Gamma_f + 2i\Gamma}. \tag{83}$$

The absolute values of the exact T-matrix elements are shown in Figs. 5(a) and 5(b) for $k_0 d = 2\pi n$, which illustrate the perfect agreement between the Markovian result $T^{\text{M}}(E)$ and the exact result in the limit $Ed, \Gamma d \ll 1$.

The Fourier transformation of S matrix leads to the wave function

$$\psi(x_c,x) = \frac{1}{2} \int dp_1 dp_2 S_{p_1 p_2, k_1 k_2} e^{ip_1 x_1 + ip_2 x_2} \tag{84}$$

of two reflected photons, where the center-of-mass coordinate $x_c = (x_1 + x_2)/2$ and the relative coordinate $x = x_1 - x_2$. For two incident photons with the same momentum $k_1 = k_2 = k$, the photon statistics is characterized by the second order correlation function

$$g^{(2)}(\tau) = \frac{|\psi(x_c,\tau)|^2}{|R_k|^4}. \tag{85}$$

In Figs. 5(c) and 5(d), we show $g^{(2)}(0)$ as the function of $E = 2k$ and $g^{(2)}(\tau)$ for the resonant frequency $k = 0$, where the Markovian results perfectly agree with the exact result in the small kd and Γd limit. When d is increasing, e.g., $\Gamma d = 0.1$ and 1, the Markovian result deviates from the exact one.

As the summary in this section, we use the exact result to study the non-Markovian effects and examine the condition of the Markov approximation. We conclude that in the limit $\Gamma N d, kN d \ll 1$, the Markov approximation works perfectly. For the large $\Gamma N d$ and $kN d$, some non-Markovian effects emerge, e.g., the retardation effect. In the following sections,

we assume the system length Nd is small enough and the Markov approximation is always valid.

VI. ENTANGLED PHOTON PAIRS BY SINGLE EMITTER

In this section, we use the scattering theory to study the generation of entangled photons in the scattering process. In order to realize the deterministic generation of reflected photons, the two-level emitter is placed at the left-hand side of a perfect mirror, i.e., in the half-end waveguide, as shown in Fig. 1(c). Here, the mirror is put at the origin, and the position of the emitter is $x_0 < 0$.

It follows from Eq. (35) that the effective action is

$$
\begin{aligned}
S_{\text{eff}} = {}& S_{\text{sys}} + i \int dt \, \Gamma e^\dagger(t) e(t) + i \int dt \, \Gamma_b b^\dagger(t) b(t) \\
& + i\sqrt{\Gamma\Gamma_b} \int dt \, b^\dagger(t) e(t+x_0) e^{-ik_0 x_0} \\
& + i\sqrt{\Gamma\Gamma_b} \int dt \, e^\dagger(t) b(t+x_0) e^{-ik_0 x_0},
\end{aligned}
\tag{86}
$$

where the emitter action S_{sys} is determined by the Hamiltonian $H_{\text{sys}} = H_{\text{emitter}}$. By the creation (annihilation) operator $e^\dagger$ (e), the hardcore boson is introduced to describe the two-level emitter, where the energy level spacing is $\omega_e = k_0$ and $H_{\text{emitter}} = U_0 e^\dagger e^\dagger e e / 2$ in the limit $U_0 \to \infty$. The external source term $S_J = -\int_{t_i}^{t_f} dt \, H_{\text{d}}(t)$ is given by Eqs. (19) and (6) with the jump operator $O = e$.

A. Single- and two-photon scattering

For the single incident photon with the momentum k and the emitter initially in the ground state, the boundary condition is $\gamma_{\text{in}} = I$ and $\mathcal{F}_{\text{in}} = \lim_{\{J_k\} \to 0} \delta / \delta J_{k,r}$ in the asymptotic limit $t_i \to -\infty$. By the boundary condition $\gamma_{\text{out}} = I$ and $\mathcal{F}_{\text{out}} = \lim_{\{J_k\} \to 0} \delta / \delta J_{p,l}$ in the asymptotic limit $t_f \to \infty$, Eqs. (14) and (34) result in the reflection coefficient

$$
\begin{aligned}
R_k \delta_{p,-k} = {}& -i \delta_{p,-k} \big[\Gamma G_{ee}(k) e^{2i(k+k_0)x_0} + \Gamma_b G_{bb}(k) \\
& + 2\sqrt{\Gamma\Gamma_b} G_{eb}(k) e^{i(k+k_0)x_0} \big],
\end{aligned}
\tag{87}
$$

where the Green's functions $G_{ss'}(k) = -i \int dt \, e^{ikt} \langle s(t) s'^\dagger \rangle$ with $s, s' = e, b$. The effective action determines the single particle Green's functions

$$
\begin{pmatrix} G_{ee}(k) & G_{eb}(k) \\ G_{be}(k) & G_{bb}(k) \end{pmatrix}
= \begin{pmatrix} k+i\Gamma & i\sqrt{\Gamma\Gamma_b}\,e^{-i(k_0+k)x_0} \\ i\sqrt{\Gamma\Gamma_b}\,e^{-i(k_0+k)x_0} & k+i\Gamma_b \end{pmatrix}^{-1},
\tag{88}
$$

which give the reflection coefficient

$$
R_k \delta_{p,-k} = -\frac{k - i\Gamma + i\Gamma e^{-2i(k+k_0)|x_0|}}{k + i\Gamma - i\Gamma e^{2i(k_0+k)|x_0|}} \delta_{p,-k}
\tag{89}
$$

and $|R_k| = 1$ in the limit $\Gamma_b \to \infty$. The phase shift $\arg(R_k)$ is shown in Fig. 6(a) for $d = 10^{-4}$, where $\theta_0 = k_0 |x_0|$.

For two incident photons with momenta k_1 and k_2 and the emitter initially in the ground state, the boundary condition
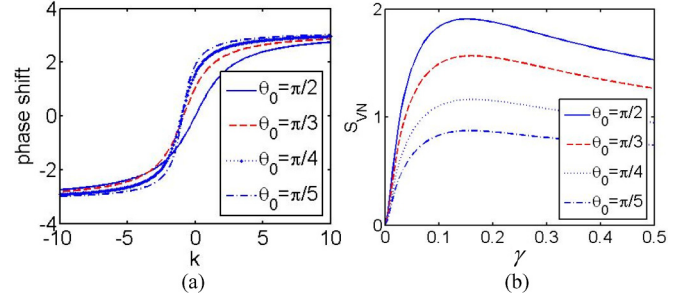
FIG. 6. (Color online) (a) The phase shift of the single photon. (b) The von Neumann entropy of the reflective photons. Here, $d = 10^{-4}$, and Γ is taken as the unit.

is $\gamma_{\text{in}} = I$ and $\mathcal{F}_{\text{in}} = \lim_{\{J_k\} \to 0} \delta^2 / \delta J_{k_1,r} \delta J_{k_2,r}$ in the asymptotic limit $t_i \to -\infty$. By the boundary condition $\gamma_{\text{out}} = I$ and $\mathcal{F}_{\text{out}} = \lim_{\{J_k\} \to 0} \delta^2 / \delta J_{-p_1,l} \delta J_{-p_2,l}$ in the asymptotic limit $t_i \to -\infty$, the S-matrix element

$$
\begin{aligned}
S_{-p_1-p_2; k_1 k_2} = {}& R_{k_1} R_{k_2} \big(\delta_{p_1 k_1} \delta_{p_2 k_2} + \delta_{p_1 k_2} \delta_{p_1 k_1} \big) \\
& - i \frac{16}{\pi} \Gamma^2 \delta_{p_1+p_2, k_1+k_2} T(E) \\
& \times \prod_{i=1,2} \frac{\sin[(k_i+k_0)|x_0|] \sin[(p_i+k_0)|x_0|]}{[k_i + i\Gamma - i\Gamma e^{2i(k_0+k_i)|x_0|}][p_i + i\Gamma - i\Gamma e^{2i(k_0+p_i)|x_0|}]}
\end{aligned}
\tag{90}
$$

of two reflected photons with momenta p_1 and p_2 is given by Eqs. (14) and (34) in the asymptotic limit $t_f \to \infty$. Here, the T-matrix element

$$
T(E) = \frac{1}{U_0^{-1} - \Pi(E)}
\tag{91}
$$

is determined by the vacuum bubble

$$
\Pi(E) = i \int \frac{d\omega}{2\pi} G_{ee}(\omega) G_{ee}(E-\omega)
\tag{92}
$$

and $E = k_1 + k_2 = p_1 + p_2$.

B. Entangled photon pairs

For the state $\sum_{k_1 k_2} f(k_1) f(k_2) r_{k_1}^\dagger r_{k_2}^\dagger |0\rangle / \sqrt{2}$ of two independent incident photons, the S matrix (90) leads to the asymptotic state

$$
|\psi_{\text{out}}\rangle = \frac{1}{\sqrt{2}} \sum_{p_1 p_2} \psi_{\text{out}}(p_1, p_2) l_{-p_1}^\dagger l_{-p_2}^\dagger |0\rangle
\tag{93}
$$

of two reflected photons, where the wave function is

$$
\begin{aligned}
\psi_{\text{out}}(p_1, p_2) = {}& f(p_1) f(p_2) R_{p_1} R_{p_2} - 16 i \Gamma^2 T(E) F_2(E) \\
& \times \prod_{i=1,2} \frac{\sin[(p_i+k_0)|x_0|]}{p_i + i\Gamma - i\Gamma e^{2i(k_0+p_i)|x_0|}},
\end{aligned}
\tag{94}
$$

and the integral

$$
F_2(E) = \int \frac{dk}{2\pi} \prod_{\sigma=\pm 1} \frac{f\left(\frac{E}{2}+\sigma k\right) \sin\left[\left(\frac{E}{2}+\sigma k+k_0\right)|x_0|\right]}{\frac{E}{2}+\sigma k + i\Gamma - i\Gamma e^{2i\left(\frac{E}{2}+\sigma k+k_0\right)|x_0|}}.
\tag{95}
$$

The von Neumann entropy $S_{VN} = -\text{tr}(\rho_1 \ln \rho_1)$ is given by the single-photon reduced density matrix $\rho_1 = \text{tr}_2(|\psi_{out}\rangle\langle\psi_{out}|)$, where the degree of freedom for the other photon is traced out. The von Neumann entropy $S_{VN} = -\sum_\lambda \lambda^2 \ln \lambda^2$ can be obtained by the singular value decomposition of $\psi_{out}(p_1, p_2) = \sum_\lambda g_\lambda(p_1)\lambda \tilde{g}_\lambda(p_2)$. Here, the singular values λ measure the entanglement of two photons in different modes g_λ and $\tilde{g}_\lambda$. For the single-photon wave packet

$$f(k) = \sqrt{\frac{\gamma}{\pi}}\frac{1}{k + i\gamma}, \tag{96}$$

we show S_{VN} in Fig. 6(b) for $d = 10^{-4}$, which displays the generation of entangled photons by the two-level emitter.

VII. RYDBERG-EIT SYSTEM

In this section, we consider the application of the scattering theory in the photon transmission in the EIT atoms coupled to the Rydberg level. We shall show that the developed scattering theory is an efficient approach to the photon transmission in the array of interacting emitters with complicated structures. Here, we highlight the interplay between the EIT phenomenon and the Rydberg interaction, and show a rich variety of quantum statistics of the scattering photons and polariton exitations.

In the rotating frame, the Hamiltonian (7) becomes

$$H_{sys} = \sum_i [\Delta_e e_i^\dagger e_i + \Delta_s s_i^\dagger s_i + (\Omega e_i^\dagger s_i + \text{H.c.})]$$
$$+ H_{HC} + \frac{1}{2}\sum_{ij} U_{ij} s_i^\dagger s_j^\dagger s_j s_i, \tag{97}$$

where $\Delta_e = \omega_e - k_0$, $\Delta_s = \omega_s - k_0 + \omega_d$, and we focus on the two-photon resonance case $\Delta_s = 0$. The waveguide photons couple to the N atoms collectively through the operator $O_{k,\pm} = \sqrt{\Gamma}\sum_{i=1}^N e^{-i(k\pm k_0)x_i}e_i/\sqrt{L}$, and the free space modes couple to the atom operator e_i locally, which induces the decay of the excited state e. The effective action

$$S_{eff} = \int dt \left\{ \sum_i [e_i^\dagger(t)(i\partial_t + i\Gamma_f)e_i(t) + |s_i^\dagger(t)i\partial_t s_i(t)] - H_{sys} \right\}$$
$$+ S_{re} \tag{98}$$

of EIT atoms is given by

$$S_{re} = i\Gamma \int dt \sum_{ij} e_i^*(t) e_j(t - |x_i - x_j|)e^{ik_0|x_i-x_j|}. \tag{99}$$

The source term $S_J = -\int_{t_i}^{t_f} dt\, H_d(t)$ is determined by Eq. (19). Here, the lattice spacing d satisfies $k_0 d = (2n + 1/2)\pi$.

Based on the general results (14) and (34), we first study the single- and two-photon scatterings, and show the transmission spectrum and the second order correlation function of outgoing photons. In the second part, we investigate the transient processes and show how the wave packets of single and two incident photons transfer to the atom excitations, propagate in the Rydberg-EIT atom array, and finally emit back to the waveguide. For the single incident photon, we show the free propagation of the dark polariton. For two incident photons,

we show the counterpropagation and copropagation of two polaritons.

A. Single- and two-photon scatterings

For the single incident photon with the momentum k and the atoms initially in the ground state, the boundary condition is $\gamma_{in} = I$ and $\mathcal{F}_{in} = \lim_{\{J_k\}\to 0} \delta/\delta J_{k,r}$ in the asymptotic limit $t_i \to -\infty$. By the boundary conditions $\gamma_{out} = I$ and $\mathcal{F}_{out} = \lim_{\{J_k\}\to 0} \delta/\delta J_{p,(r,l)}$ in the asymptotic limit $t_f \to \infty$, Eqs. (14) and (34) lead to the reflection and transmission coefficients

$$R_k \delta_{p,-k} = -i\Gamma \delta_{p,-k} \sum_{ij} [G_0(k)]_{ij}^{ee} e^{i(k+k_0)(x_i+x_j)},$$
$$\tag{100}$$
$$T_k \delta_{p,k} = \delta_{pk}\left\{ 1 - i\Gamma \sum_{ij} [G_0(k)]_{ij}^{ee} e^{-i(k+k_0)(x_i-x_j)} \right\}$$

of the photon with momentum p.

The free Green's function

$$G_0(\omega) = \frac{1}{\omega - \mathcal{H}_0(\omega)} \tag{101}$$

of atoms is determined by the block form

$$\mathcal{H}_0(\omega) = \begin{pmatrix} (\Delta_e - i\Gamma_f)\delta_{ij} - i\Gamma e^{i(k_0+\omega)|x_i-x_j|} & \Omega\delta_{ij} \\ \Omega\delta_{ij} & \Delta_s\delta_{ij} \end{pmatrix} \tag{102}$$

in the basis $|e_i\rangle$ and $|s_i\rangle$, where each matrix element is the N-dimensional matrix in the coordinate basis. In the notation $[G_0(k)]_{ij}^{\sigma\sigma'}$, $\sigma(\sigma') = e,s$ denotes the different "spin" blocks and i, j denote the coordinate in the block. In the Markov limit $\omega d \ll 1$, $\mathcal{H}_0(\omega)$ is approximated by the frequency independent effective Hamiltonian

$$\mathcal{H}_0^M = \begin{pmatrix} (\Delta_e - i\Gamma_f)\delta_{ij} - i\Gamma e^{ik_0|x_i-x_j|} & \Omega\delta_{ij} \\ \Omega\delta_{ij} & \Delta_s\delta_{ij} \end{pmatrix}, \tag{103}$$

In Fig. 7, the exact transmission probability is compared with that under the Markov approximation. As shown in Figs. 7(a) and 7(b), for the small lattice spacing $d = 10^{-4}$, the Markov approximation works very well, which leads to the same result as that from Eq. (102). When the lattice spacing $d = 10^{-2}$ is larger, Fig. 7(c) shows the difference between the results under the Markov approximation (103) and the exact result (102). In the realistic case, the small length of the array justifies the validity of the Markov approximation. Henceforth, we focus on the Markov limit. In Figs. 7(b) and 7(d), we have taken into account the decay of the excited state $|e_i\rangle$ to the free space, i.e., $\Gamma_f \neq 0$. The single-photon transmission shows the EIT nature of atoms, where the total transmission appears at the resonant frequency $k = 0$ in the EIT window. The reason for the total transmission is that the resonant photon transforms to the free-propagating dark polariton excitation, which is only the superposition of states $r_k^\dagger|g_i\rangle$ and $|s_i\rangle$. As a result, the free space decay Γ_f of the state $|e_i\rangle$ does not affect the total transmission of the resonant dark polariton with $k = 0$.

For the two incident photons with momenta k_1 and k_2 and the atoms initially in the ground state, the initial boundary
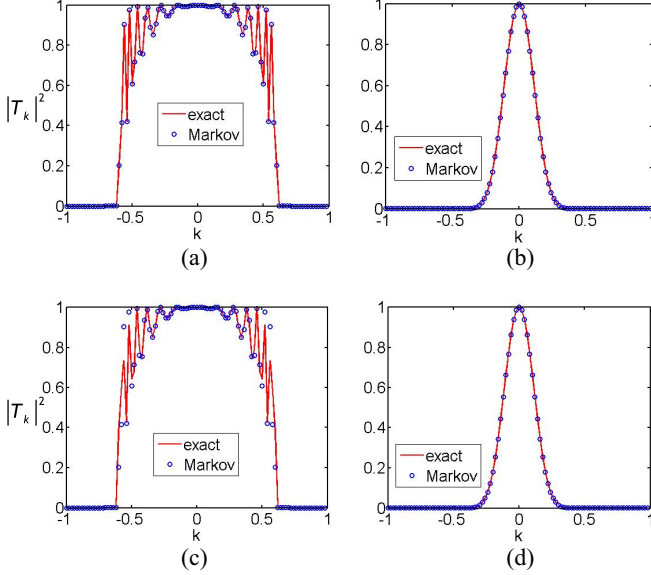
FIG. 7. (Color online) The single-photon transmission spectra, where $\Gamma = 1$, $\Delta_e = 0$, $\Omega = 1$, and the atom number is 20. (a) $\Gamma_f = 0$ and $d = 10^{-4}$; (b) $\Gamma_f = 1$ and $d = 10^{-4}$; (c) $\Gamma_f = 0$ and $d = 10^{-2}$; (d) $\Gamma_f = 1$ and $d = 10^{-2}$.

condition is $\gamma_{\text{in}} = I$ and $\mathcal{F}_{\text{in}} = \lim_{\{J_k\} \to 0} \delta^2 / \delta J_{k_1,r} \delta J_{k_2,r}$ in the asymptotic limit $t_i \to -\infty$. By the boundary condition of the final state $\gamma_{\text{out}} = I$ and $\mathcal{F}_{\text{out}} = \lim_{\{J_k\} \to 0} \delta^2 / \delta J_{p_1,r} \delta J_{p_2,r}$ in the asymptotic limit and $t_f \to \infty$, Eqs. (14) and (34) lead to the two-photon S matrix

$$S_{p_1 p_2; k_1 k_2} = T_{k_1} T_{k_2} \left(\delta_{p_1 k_1} \delta_{p_2 k_2} + \delta_{p_1 k_2} \delta_{p_2 k_1} \right)$$
$$+ \frac{\Gamma^2}{(2\pi)^2} \sum_{i_1 i_2, j_1 j_2} e^{i k_0 (x_{j_1} + x_{j_2} - x_{i_1} - x_{i_2})}$$
$$\times G_{i_1 i_2; j_1 j_2}^{ee;ee}(p_1, p_2; k_1, k_2) \tag{104}$$

for two transmitted photons with momenta p_1 and p_2. Here, the Green's function

$$G_{i_1 i_2; j_1 j_2}^{ee;ee}(p_1, p_2; k_1, k_2) = \int dt_1' dt_2' dt_1 dt_2 e^{i p_1 t_1' + i p_2 t_2' - i k_1 t_1 - i k_2 t_2}$$
$$\times \left\langle \mathcal{T} e_{i_1}(t_1') e_{i_2}(t_2') e_{j_1}^\dagger(t_1) e_{j_2}^\dagger(t_2) \right\rangle_c \tag{105}$$

is the Fourier transformation of the four-point connected Green's function.

The Dyson expansion in terms of the two-body interaction $H_{\text{HC}} + \sum_{ij} U_{ij} s_i^\dagger s_j^\dagger s_j s_i / 2$ leads to

$$S_{p_1 p_2; k_1 k_2} = S_{p_1 p_2; k_1 k_2}^{(0)} - i \frac{\Gamma^2}{2\pi} \delta_{p_1 + p_2, k_1 + k_2}$$
$$\times \sum_{\substack{i j i' j' \\ \sigma_1 \sigma_1' \sigma_2 \sigma_2'}} [w^*(p_1, p_2)]_{ij}^{\sigma_1 \sigma_1'} [T(E)]_{ij;i'j'}^{\sigma_1 \sigma_1'; \sigma_2 \sigma_2'}$$
$$\times [w(k_1, k_2)]_{i'j'}^{\sigma_2 \sigma_2'} + (p_1 \leftrightarrow p_2), \tag{106}$$
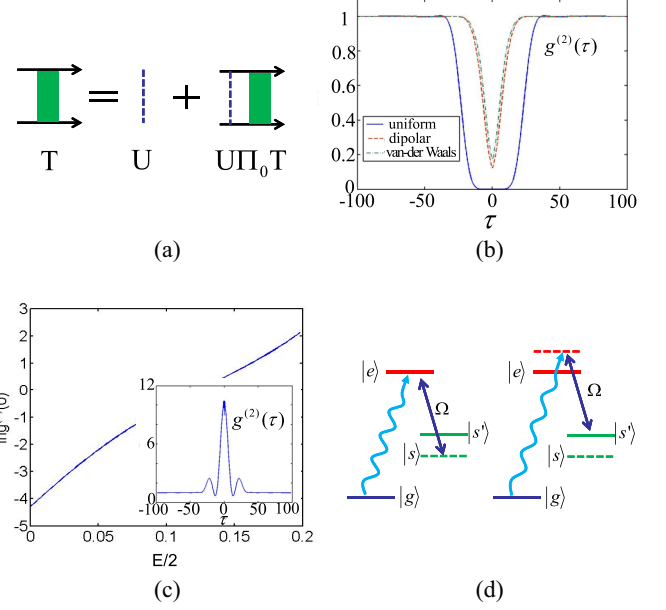
FIG. 8. (Color online) Bunching and antibunching behaviors of transmitted photons, where $\Gamma = 1$, $\Gamma_f = 1$, $\Delta_e = 0$, $\Omega = 1$, $k_0 d = \pi/2$, $U_0 = 10^8$, and the atom number is 20: (a) the Feynman diagram for the T matrix; (b) the second order correlation functions $g^{(2)}(x)$ for $C = C_3 = C_6 = 1$, $E = 0$, and $k = 0$; (c) the second order correlation functions $\ln g^{(2)}(0)$ for the uniform case $C = 0.46$, where the relative momentum $k = 0$, and the inset shows $g^{(2)}(x)$ for the frequency $E/2 = 0.2$ of each photon; (d) the schematic for the generation of the bunched and antibunched photons, where the incident photons have different frequencies. s' is the shifted energy level due to the Rydberg interaction.

where we define the independent scattering part $S_{p_1 p_2; k_1 k_2}^{(0)} = T_{k_1} T_{k_2} \delta_{p_1 k_1} \delta_{p_2 k_2}$, and the function

$$[w(k_1, k_2)]_{i'j'}^{\sigma \sigma'} = \sum_{j_1 j_2} e^{i k_0 (x_{j_1} + x_{j_2})} [G_0(k_1)]_{i' j_1}^{\sigma e} [G_0(k_2)]_{j' j_2}^{\sigma' e}. \tag{107}$$

The T matrix, depicted by the ladder diagram in Fig. 8(a), satisfies the Lippmann-Schwinger equation

$$[T(E)]_{ij;i'j'}^{\sigma_1 \sigma_1'; \sigma_2 \sigma_2'}$$
$$= U_{ij}^{\sigma_1 \sigma_1'} \delta_{i'i} \delta_{j'j} \delta_{\sigma_1 \sigma_2} \delta_{\sigma_1' \sigma_2'}$$
$$+ U_{ij}^{\sigma_1 \sigma_1'} \sum_{i_1 j_1; \mu_1 \mu_1'} [\Pi(E)]_{ij;i_1 j_1}^{\sigma_1 \sigma_1'; \mu_1 \mu_1'} [T(E)]_{i_1 j_1; i'j'}^{\mu_1 \mu_1'; \sigma_2 \sigma_2'}, \tag{108}$$

where the vacuum bubble is

$$[\Pi(E)]_{ij;i'j'}^{\sigma \sigma'; \mu \mu'} = i \int \frac{d\omega}{2\pi} [G_0(\omega)]_{ii'}^{\sigma \mu} [G_0(E - \omega)]_{jj'}^{\sigma' \mu'}. \tag{109}$$

In the matrix form, the Lippmann-Schwinger equation is formally solved as

$$T(E) = \frac{1}{\mathbf{U}^{-1} - \Pi(E)}, \tag{110}$$

where the vacuum bubble $\Pi_0(E) = (E - \mathcal{H}_2)^{-1}$ is given by $\mathcal{H}_2 = \mathcal{H}_0^{\text{M}} \otimes I_{2N} + I_{2N} \otimes \mathcal{H}_0^{\text{M}}$, and the interaction matrix $\mathbf{U}$

has the diagonal element $U_{ij}^{ee} = U_{ij}^{es} = U_{ij}^{se} = U_0 \to \infty$ and $U_{ij}^{ss} = U_{ij}$ in the basis $\{|e_i e_j\rangle, |e_i s_j\rangle, |s_i e_j\rangle, |s_i s_j\rangle\}$.

The wave function

$$\psi(x_c, x)$$

$$= \int \frac{dp_1 dp_2}{2\pi} S_{p_1 p_2; k_1 k_2} e^{ip_1 x_1 + ip_2 x_2}$$

$$= \frac{e^{iEx_c}}{2\pi} \left\{ 2 T_{(E/2)+k} T_{(E/2)-k} \cos(kx) - i\Gamma^2 \sum_{\substack{iji'j' \\ \sigma\sigma'\mu\mu'}} [F(x)]_{ij}^{\sigma\sigma'} \right.$$

$$\left. \times [T(E)]_{ij;i'j'}^{\sigma\sigma';\mu\mu'} \left[w \left(\frac{E}{2} + k, \frac{E}{2} - k \right) \right]_{i'j'}^{\mu\mu'} \right\} \quad (111)$$

of two transmitted photons is the Fourier transform of $S_{p_1 p_2; k_1 k_2}$, where

$$[F(x)]_{ij}^{\sigma\sigma'} = -i \sum_{i_1 i_2} \frac{e^{-ik_0 x_{c,12}}}{E - \varepsilon_l - \varepsilon_{l'}} \sum_{ll'} \chi_l(i_1 e) \chi_{l'}(i_2 e)$$

$$\times \tilde{\chi}_l^*(i\sigma) \tilde{\chi}_{l'}^*(j\sigma')[e^{i[(E/2)-\varepsilon_{l'}]x} \theta(x)$$

$$+ e^{-i[(E/2)-\varepsilon_l]x} \theta(-x)] + (x \to -x) \quad (112)$$

is determined by $x_{c,12} = x_{i_1} + x_{i_2}$ and the eigenstates $|\chi_l\rangle$ ($|\tilde{\chi}_l\rangle$) of $\mathcal{H}_0^M$ ($\mathcal{H}_0^{M\dagger}$) with the corresponding eigenenergies ε_l (ε_l^*). Here, $\langle i\sigma|\chi_l\rangle = \chi_l(i\sigma)$ and $\langle i\sigma|\tilde{\chi}_l\rangle = \tilde{\chi}_l(i\sigma)$.

By the wave function (111), we show the normalized second order correlation function $g^{(2)}(x) = |\pi\psi(x_c, x)/T_{E/2}^2|^2$ of outgoing photons for the two incident photons with the same momentum $k_1 = k_2 = E/2$ in Figs. 8(b) and 8(c). For the resonant case $E = 0$, Fig. 8(b) shows the second order correlation functions for the uniform interaction $U_{ij}^{ss} = C$, the van der Waals interaction $U_{ij}^{ss} = C_6/|i - j|^6$, and the dipolar interaction $U_{ij}^{ss} = C_3/|i - j|^3$, which exhibit the antibunching behavior of outgoing photons.

It can be understood in the following way. As shown in the left panel of Fig. 8(d), if two Rydberg excitations are close to each other, the Rydberg state is shifted by the strong Rydberg interaction, such that the classical light is off-resonant with respect to the transition between $|e_i\rangle$ and $|s_i\rangle$. As a result, the photon with $k = 0$ is resonant with the transition $|g_i\rangle \to |e_i\rangle$ and reflected. For two transmitted photons, to maintain that the frequency $k = 0$ of the photon is in the EIT transmission window, they repulse each other and show the antibunching behavior such that the Rydberg state is not shifted.

For the incident photons with frequency $E/2$ larger than some critical value, the transmitted photons can also display bunching behavior, as shown in Fig. 8(c). The mechanism of the generation of bunched photons is illustrated in the right panel of Fig. 8(d). For two Rydberg excitations close to each other, the Rydberg energy levels $|s_i\rangle$ are shifted. The photons with finite momentum $E/2$ realize the two-photon resonance with the shifted energy level $|s_i\rangle$, and can be transmitted. In order to achieve the transmission of photons by the shifted Rydberg levels $|s_i\rangle$, the two Rydberg excitations prefer to stay next to each other, which induces the bunching behavior of the transmitted photons.

As discussed in Sec. III, the second order correlation function $g^{(2)}(x)$ obtained by the scattering theory can characterize

the quantum statistics of photons emitted by the Rydberg-EIT atoms under the weak driving field. In Ref. [42], the result from the scattering theory and the numerical solution of the master equation for the effective spin model under the weak driving light are compared, where the two results agree with each other perfectly.

B. Propagations of single and two excitations

In this section, we investigate how the single and two incident photons transform to the excitations of the Rdyberg atoms, and the propagation of excitations.

For the single incident photon with the wave packet $f(k)$ and the atoms initially in the ground state, the boundary condition is $\gamma_{in} = I$ and $\mathcal{F}_{in} = \sum_k f_{(r,l)}(k) \lim_{\{J_k\} \to 0} \delta/\delta J_{k,(r,l)}$ at the instant $t_i = 0$, where the wave packets of the right- and left-moving photons are

$$f(k) = f_r(k) = \sqrt{\frac{\gamma}{\pi}} \frac{1}{k + i\gamma} \quad (113)$$

and

$$f(k) = f_l(k) = \sqrt{\frac{\gamma}{\pi}} \frac{e^{-ikx_N}}{k - i\gamma}, \quad (114)$$

with the width $1/\gamma$. By the final boundary conditions $\mathcal{F}_{out} = 1$ and $\gamma_{out} = \mu_i = e_i, s_i$ at the instant $t_f = T$, Eqs. (14) and (34) lead to the amplitude

$$\mathcal{A}_{i\mu}^{(\alpha)}(T) = i\sigma_\alpha \sqrt{2\gamma\Gamma} \sum_{lj} e^{i\sigma_\alpha k_0 x_j} \theta(T_\alpha - \sigma_\alpha x_j)$$

$$\times \frac{\chi_l(i\mu)\tilde{\chi}_l^*(je)}{\varepsilon_l + i\gamma} [e^{-\gamma(T_\alpha - \sigma_\alpha x_j)} - e^{-i\varepsilon_l(T_\alpha - \sigma_\alpha x_j)}]$$

$$(115)$$

of the excitation $\mu = e, s$ at the position i, where $T_\alpha = T - z_\alpha$ and $z_r = 0$, $z_l = x_N$. For this situation, the dark polariton forms, where the probability of the occupation in the excited state $|e_i\rangle$ is quite small, $\sim 10^{-4}$. In Fig. 9, we show the dark polariton propagation for the single right-moving incident photon. In order to show the slow propagation of the dark polariton, we choose the small ratio $\Omega/\Gamma = 0.1$.

For the wave packet of two incident photons and the atoms initially in the ground state, we consider both the copropagation and counterpropagation cases. For the copropagation, the
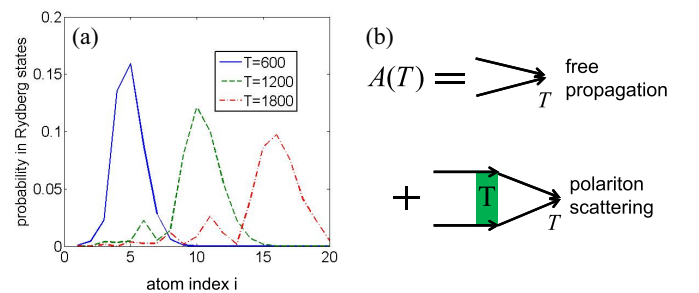
FIG. 9. (Color online) (a) Probability of Rydberg states for the single incident photon wave packet, where $\Gamma = 1$, $\Gamma_f = 0$, $\Delta = 0$, $\Omega = 0.1$, $d = 10^{-4}$, $\gamma = 0.01$, and the atom number is 20. (b) The Feynman diagram for the two excitation propagation.

initial boundary condition at the instant $t_i = 0$ is $\gamma_{\rm in} = I$ and

$$\mathcal{F}_{\rm in} = \sum_{k_1 k_2} f_r(k_1) f_r(k_2) \lim_{\{J_k\} \to 0} \frac{\delta^2}{\delta J_{k_1,r} \delta J_{k_2,r}}, \qquad (116)$$

while for the counterpropagation, the initial boundary condition at the instant $t_i = 0$ is $\gamma_{\rm in} = I$ and

$$\mathcal{F}_{\rm in} = \sum_{k_1 k_2} f_r(k_1) f_l(k_2) \lim_{\{J_k\} \to 0} \frac{\delta^2}{\delta J_{k_1,r} \delta J_{k_2,l}}. \qquad (117)$$

By the boundary condition $\mathcal{F}_{\rm out} = 1$ and $\gamma_{\rm out} = \mu_{1,i_1} \mu_{2,i_2}$ ($\mu_{1,2} = e,s$) at the instant $t_f = T$, Eqs. (14) and (34) result in the amplitude

$$\mathcal{A}_{i_1 i_2; \mu_1 \mu_2}^{(r,\alpha)}(T)$$

$$= \mathcal{P}_{i_1 \mu_1; i_2 \mu_2} \left\{ \mathcal{A}_{i_1 \mu_1}^{(r)}(T) \mathcal{A}_{i_2 \mu_2}^{(\alpha)}(T) + 2\gamma \Gamma \sigma_\alpha \sum_{j_1 j_2} e^{i k_0 x_{j_1} + i \sigma_\alpha k_0 x_{j_2}} \right.$$

$$\times \theta(T - x_{j_1}) \theta(T - z_\alpha - \sigma_\alpha x_{j_2}) \int \frac{d\omega_1}{2\pi} \int \frac{d\omega_2}{2\pi}$$

$$\times \sum_{i'j',\sigma\sigma'} \left[\frac{1}{\omega_1 + \omega_2 - \mathcal{H}_2} \right]_{i_1 i_2; ij}^{\mu_1 \mu_2; \sigma\sigma'} \mathbf{U}_{ij}^{\sigma\sigma'} [G(\omega_1)]_{ij_1}^{\sigma e}$$

$$\times [G(\omega_2)]_{jj_2}^{\sigma' e} \frac{e^{-i\omega_1(T - x_{j_1})}}{\omega_1 + i\gamma} \frac{e^{-i\omega_2(T - z_\alpha - \sigma_\alpha x_{j_2})}}{\omega_2 + i\gamma} \left. \right\} \qquad (118)$$

of two excitations μ_1 and μ_2 at the positions i_1 and i_2 for the copropagation $\alpha = r$ and the counterpropagation $\alpha = l$ case, where the operator $\mathcal{P}_{i_1 \mu_1; i_2 \mu_2}$ symmetrizes the wave function under the interchange $i_1 \mu_1 \longleftrightarrow i_2 \mu_2$.

In the first row of Fig. 10, we show the propagation of two dark polaritons for two counterpropagating incident photons.
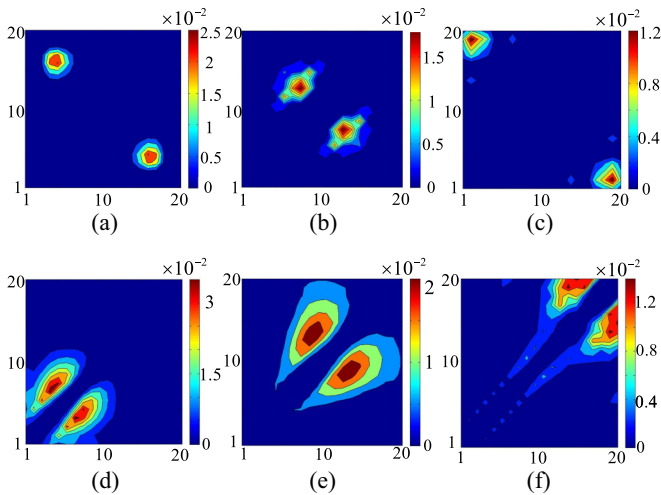
FIG. 10. (Color online) Probabilities in the state $|s\rangle$ for two counter- and copropagating polaritons with the dipolar case $C_3 = 1$, where $\Gamma = 1$, $\Gamma_f = 0$, $\Delta_e = 0$, $d = 10^{-4}$, and the atom number is 20. (a)–(c) show the probabilities at the instants $T = 600$, 1200, and 1800 for the counterpropagation case: $\Omega = 0.1$ and $\gamma = 0.01$; (d)–(f) show the probabilities at the instants $T = 12$, 20, and 28 for the copropagation case: $\Omega = 1$ and $\gamma = 0.1$.

Here, we choose $\Omega/\Gamma = 0.1$ to show the collision of two slow polaritons. When the two excitations approach each other, the states $|s_i\rangle$ are shifted by the Rydberg interaction, which results in the off-resonance with the transition from $|e_i\rangle$ to $|s_i\rangle$ induced by the classical light. As a result, the photon is resonant with the excited state $|e_i\rangle$ and reflected. After the collision of two excitations, they propagate away from each other, and the interaction gradually vanishes, which results in the reformation of two free propagating dark polaritons.

In the second row of Fig. 10, the propagation of two dark polaritons for the copropagation incident photons is shown. When the first photon transforms into the dark polariton in the atom array, it blocks the transmission of the second photon. This blockade occurs over a characteristic distance $r_b \sim (C_3 \Gamma / \Omega^2)^{1/3}$. For an incoming two-photon wave packet whose size is larger than r_b, the blockade manifests itself as a suppression of the probability of two photons to overlap with each other as they propagate through the medium [see Figs. 10(d)–10(f)]. During the propagation in the Rydberg-EIT atoms, the two polaritons keep away from each other such that the energy levels $|s_i\rangle$ are not shifted, which results in the transmission of two antibunched dark polaritons.

VIII. CONCLUSION

We summarize our results in this section. We developed the scattering theory to investigate propagation of photons through an array of quantum emitters using the path integral approach. The exact transition amplitude for arbitrary initial and final states is obtained to describe the quantum statistics of scattering photons and the dynamics of emitters in the transient process. The exact result justifies the correctness of the Markov approximation for the single emitter coupled to the waveguide photons with linear dispersion. The exact and Markovian results coincide when the bandwidth of the dynamics is sufficiently small compared to the distance between emitters. Here, the generalized master equation for the few-photon scattering process is obtained to describe the transient dynamics of emitters. The generalized master equation establishes the relation between two equivalent systems, i.e., few photon scattering by the emitters and the emitters under weak driving light.

For the single emitter case, two paradigmatic examples, i.e., the two-level emitter and the JC system, are used to show the correctness of our theory by comparison with the well-known results. For an array of emitters, the validity of the Markov approximation is examined in the system with two-level emitters coupled to waveguide photons. Here, the dynamical evolution of emitters show some non-Markovian effects, i.e., the retardation effect.

The generation of entangled photons by the single emitter in front of the mirror is also analyzed by the exact result from our theory. Finally, the photon transmission in an array of EIT atoms coupled to the Rydberg level is investigated by the scattering theory. We highlight the interplay between the EIT phenomenon and the Rydberg interaction, and show how this results in the bunching and antibunching behaviors of the scattering photons and the dark polaritons propagating in the array.

The scattering theory also provides a way to explore some non-Markovian effects of emitters coupled to the waveguide with nonlinear spectrum, where the multiphoton bound states [59,60] may form. The general result of the transition amplitude and the generalized master equation enable us to study the photon transmission in more complicated quantum optics systems and the dissipative many-body systems.

APPENDIX: GENERALIZED MASTER EQUATION BY PATH INTEGRAL

In this Appendix, we derive the generalized master equation (26) by the path integral approach. To simplify the notation, we neglect the term H_{Γ_f} describing the independent decay of each emitter to the free space, and the derivation including the free space mode follows the same procedure. In the end, we show the result by considering the effect of the free space decay.

Here, we need to introduce the emitter field explicitly. In quantum optics systems, the emitter operators are usually the annihilation (creation) operators of bosonic modes and the ladder operators. If one use the hardcore boson to describe the emitters, all the operators are bosonic operators (b_l), where l denotes the different modes of the emitters. In the coherent basis, the reduced density operator $\rho_s(T) = Tr_{\text{bath}}[e^{-iHT}\rho(0)e^{iHT}]$ becomes $\rho_s(T) = \mathcal{F}_{\text{in},-}^* \mathcal{F}_{\text{in},+} e^{\sum_{k,\alpha} J_{k,\alpha,-}^* J_{k,\alpha,+}} \rho_J(T)$:

$$
\begin{aligned}
\rho_J(T) = \int & d\mu(\beta_{l,+,\text{out}}, \beta_{l,+,\text{out}}^*) d\mu(\beta_{l,-,\text{out}}, \beta_{l,-,\text{out}}^*) \\
& \times e^{-\sum_{k,\alpha} J_{k,\alpha,-}^* J_{k,\alpha,+}} \rho_J(\beta_{l,+,\text{out}}^*, \beta_{l,-,\text{out}}; T) \\
& \times |\{\beta_{l,+,\text{out}}\}\rangle\langle\{\beta_{l,-,\text{out}}\}|,
\end{aligned} \tag{A1}
$$

where $\alpha = r,l$ denotes the right- and left-moving photon modes,

$$
\mathcal{F}_{\text{in},\pm} = \lim_{\{J_{k\alpha}\}\to 0} \sum_{\{n_{k\alpha}\}} \psi_{\text{in}}(\{n_{k\alpha}\}) \prod_{k\alpha} \frac{1}{\sqrt{n_{k\alpha}!}} \frac{\delta^{n_{k\alpha}}}{\delta J_{k,\alpha,\pm}^{n_{k\alpha}}}, \tag{A2}
$$

the measure for the unnormalized coherent state $|\{\beta_l\}\rangle$ is $d\mu(\beta_l, \beta_l^*) = \prod_l (e^{-|\beta_l|^2} d^2\beta_l/\pi)$, and the element

$$
\begin{aligned}
& \rho_J(\beta_{l,+,\text{out}}^*, \beta_{l,-,\text{out}}; T) \\
& = \int d\mu(\beta_{l,\pm,\text{in}}, \beta_{l,\pm,\text{in}}^*) \\
& \quad \times Z_J(\beta_{l,+,\text{out}}^*, \beta_{l,-,\text{out}}; \beta_{l,+,\text{in}}, \beta_{l,-,\text{in}}^*; T)\rho_0(\beta_{l,+,\text{in}}^*, \beta_{l,-,\text{in}})
\end{aligned}
$$

is given by the propagator

$$
\begin{aligned}
& Z_J(\beta_{l,+,\text{out}}^*, \beta_{l,-,\text{out}}; \beta_{l,+,\text{in}}, \beta_{l,-,\text{in}}^*; T) \\
& = \int d\mu(J_{k,\alpha}, J_{k,\alpha}^*)\langle\{J_{k,\alpha}\}|\langle\{\beta_{l,+,\text{out}}\}|e^{-iHT}|\{\beta_{l,+,\text{in}}\}\rangle \\
& \quad \times |\{J_{k,\alpha,+}\}\rangle\langle\{J_{k,\alpha,-}\}|\langle\{\beta_{l,-,\text{in}}\}|e^{iHT}|\{\beta_{l,-,\text{out}}\}\rangle|\{J_{k,\alpha}\}\rangle
\end{aligned} \tag{A3}
$$

in the closed time path. Here, we define $\rho_0(\beta_{l,+,\text{in}}^*, \beta_{l,-,\text{in}}) = \langle\{\beta_{l,+,\text{in}}\}|\rho_{\text{sys}}(0)|\{\beta_{l,-,\text{in}}\}\rangle$.

The propagator (A3) is obtained by the saddle-point method shown in Sec. III C, which is

$$
\begin{aligned}
& Z_J(\beta_{l,+,\text{out}}^*, \beta_{l,-,\text{out}}; \beta_{l,+,\text{in}}, \beta_{l,-,\text{in}}^*; T) \\
& = e^{iS_b} \int d\mu(J_{k,\alpha}, J_{k,\alpha}^*) \\
& \quad \times \exp\left\{\sum_{k,\alpha=r,l} [J_{k,\alpha}^* J_{k,\alpha,+} e^{-i\sigma_\alpha kT} + J_{k,\alpha,-}^* J_{k,\alpha} e^{i\sigma_\alpha kT}]\right\} \\
& \quad \times \int D[\text{system}] e^{iS_{\text{eff},+} - iS_{\text{eff},-}^* + iS_{J,+} - iS_{J,-}^*}.
\end{aligned} \tag{A4}
$$

Here, $iS_b = \sum_l [\beta_{l,+,\text{out}}^* \beta_l(T) + \beta_l^*(T)\beta_{l,-,\text{out}}]$ is the boundary term for the emitters, and $S_{\text{eff},\pm}$ are the effective actions in the forward and backward time-evolution paths, which are given by substituting the fields $\beta_{l,\pm}$ for the emitter fields in the effective action S_{eff}. The external source term is

$$
\begin{aligned}
S_{J,\pm} = -\int_0^T dt \sum_{k,\alpha} \big[& J_{k,\alpha}^* O_{k,\sigma_\alpha,\pm}(t) e^{-i\sigma_\alpha k(T-t)} \\
& + J_{k,\alpha,\pm} O_{k,\sigma_\alpha,\pm}^*(t) e^{-i\sigma_\alpha kt} \big].
\end{aligned} \tag{A5}
$$

Finally, the Gaussian integral over $J_{k,\alpha}, J_{k,\alpha}^*$ leads to the propagator

$$
\begin{aligned}
& Z_J(\beta_{l,+,\text{out}}^*, \beta_{l,-,\text{out}}; \beta_{l,+,\text{in}}, \beta_{l,-,\text{in}}^*; T) \\
& = e^{\sum_{k,\alpha} J_{k,\alpha,-}^* J_{k,\alpha,+}} \int D[\text{system}] e^{i(S_{\text{d},+} - S_{\text{d},-} + S_{\text{jump}})} \\
& \quad \times \exp\left\{\sum_l [\beta_{l,+,\text{out}}^* \beta_l(T) + \beta_l^*(T)\beta_{l,-,\text{out}}]\right\}, \tag{A6}
\end{aligned}
$$

where

$$
\begin{aligned}
S_{\text{d},+} = S_{\text{eff},+} - \int_0^T dt \sum_{k,\alpha} \big[& J_{k,\alpha,-}^* O_{k,\sigma_\alpha,+}(t) e^{i\sigma_\alpha kt} \\
& + J_{k,\alpha,+} O_{k,\sigma_\alpha,+}^*(t) e^{-i\sigma_\alpha kt} \big],
\end{aligned} \tag{A7}
$$

$$
\begin{aligned}
S_{\text{d},-} = S_{\text{eff},-}^* - \int_0^T dt \sum_{k,\alpha} \big[& J_{k,\alpha,-}^* O_{k,\sigma_\alpha,-}(t) e^{i\sigma_\alpha kt} \\
& + J_{k,\alpha,+} O_{k,\sigma_\alpha,-}^*(t) e^{-i\sigma_\alpha kt} \big],
\end{aligned} \tag{A8}
$$

and the jump term

$$
S_{\text{jump}} = -i \int dt\, dt' \sum_{k,\alpha} e^{i\sigma_\alpha k(t-t')} O_{k,\sigma_\alpha,+}(t) O_{k,\sigma_\alpha,-}^*(t'). \tag{A9}
$$

Under the Markov approximation, the actions read

$$S_{\text{eff},\pm} = S_{\text{sys},\pm} + i \int_{t_i}^{t_f} dt \sum_{ij} \sqrt{\Gamma_i \Gamma_j}$$
$$\times O_{i,\pm}^*(t) O_{j,\pm}(t) e^{ik_0|x_i - x_j|} \qquad (A10)$$

and

$$S_{\text{jump}} = -2i \int_0^T dt \sum_{ij} \sqrt{\Gamma_i \Gamma_j} \cos[k_0(x_i - x_j)]$$
$$\times O_{i,+}(t) O_{j,-}^*(t). \qquad (A11)$$

By taking the time derivative of Eq. (A1) and using Eq. (A6), we obtain the motion equation

$$\partial_T \rho_J(T) = -i[\tilde{H}_{\text{sys}}(T), \rho_J(T)] + \mathcal{L}\rho_J(T) \qquad (A12)$$

for the generating density matrix $\rho_J(T)$ with the initial condition $\rho_J(0) = \rho_{\text{sys}}(0)$, where the Lindblad term is

$$\mathcal{L}\rho_J(T) = 2 \sum_{ij} \sqrt{\Gamma_i \Gamma_j} O_i \rho_J(T) O_j^\dagger \cos[k_0(x_i - x_j)]$$
$$- \sum_{ij} \sqrt{\Gamma_i \Gamma_j} \cos[k_0(x_i - x_j)] \{O_i^\dagger O_j, \rho_J(T)\}. \qquad (A13)$$

Finally, by adding the Lindblad term describing the free space decay, we reproduce the results (26), (27), and (28).

[1] A. Imamoğlu, H. Schmidt, G. Woods, and M. Deutsch, Phys. Rev. Lett. **79**, 1467 (1997).

[2] K. M. Birnbaum, A. Boca, R. Miller, A. D. Boozer, T. E. Northup, and H. J. Kimble, Nature (London) **436**, 87 (2005).

[3] D. E. Chang, A. S. Sørensen, E. A. Demler, and M. D. Lukin, Nat. Phys. **3**, 807 (2007).

[4] D. E. Chang, V. Vuletić, and M. D. Lukin, Nat. Photonics **8**, 685 (2014).

[5] A. González-Tudela, V. Paulisch, D. E. Chang, H. J. Kimble, and J. I. Cirac, Phys. Rev. Lett. **115**, 163603 (2015).

[6] Z. Yuan, B. E. Kardynal, R. M. Stevenson, A. J. Shields, C. J. Lobo, K. Cooper, N. S. Beattie, D. A. Ritchie, and M. Pepper, Science **295**, 102 (2005).

[7] B. Darquié, M. P. A. Jones, J. Dingjan, J. Beugnon, S. Bergamini, Y. Sortais, G. Messin, A. Browaeys, and P. Grangier, Science **309**, 454 (2005).

[8] A. J. Shields, Nat. Photonics **1**, 215 (2007).

[9] P. Michler, A. Kiraz, C. Becher, W. V. Schoenfeld, P. M. Petroff, L. Zhang, E. Hu, and A. Imamoğlu, Science **290**, 2282 (2000).

[10] T. G. Tiecke, J. D. Thompson, N. P. de Leon, L. R. Liu, V. Vuletić, and M. D. Lukin, Nature (London) **508**, 241 (2014).

[11] T. Volz, A. Reinhard, M. Winger, A. Badolato, K. J. Hennessy, E. L. Hu, and A. Imamoğlu, Nat. Photonics **6**, 605 (2012).

[12] L. Zhou, Z. R. Gong, Y. X. Liu, C. P. Sun, and F. Nori, Phys. Rev. Lett. **101**, 100501 (2008).

[13] T. G. Walker, Nature (London) **488**, 39 (2012).

[14] I. A. Walmsley and M. G. Raymer, Science **307**, 1733 (2005).

[15] H. J. Kimble, Nature (London) **453**, 1023 (2008).

[16] T. C. H. Liew and V. Savona, Phys. Rev. Lett. **104**, 183601 (2010).

[17] A. Majumdar, M. Bajcsy, A. Rundquist, and J. Vučković, Phys. Rev. Lett. **108**, 183601 (2012).

[18] M. O. Scully and M. S. Zubairy, *Quantum Optics* (Cambridge University Press, Cambridge, UK, 1997).

[19] C. S. Muñoz, E. d. Valle, A. G. Tudela, K. Müller, S. Lichtmannecker, M. Kaniber, C. Tejedor, J. J. Finley, and F. P. Laussy, Nat. Photonics **8**, 550 (2014).

[20] Y. Chang, A. G. Tudela, C. S. Muñoz, C. N. Benlloch, and T. Shi, arXiv:1510.07307.

[21] J. T. Shen and S. Fan, Phys. Rev. Lett. **98**, 153003 (2007).

[22] T. Shi and C. P. Sun, Phys. Rev. B **79**, 205111 (2009).

[23] T. Shi, S. Fan, and C. P. Sun, Phys. Rev. A **84**, 063803 (2011).

[24] M. Bamba, A. Imamoğlu, I. Carusotto, and C. Ciuti, Phys. Rev. A **83**, 021802(R) (2011).

[25] T. Shi and S. Fan, Phys. Rev. A **87**, 063818 (2013).

[26] C. Kurtsiefer, S. Mayer, P. Zarda, and H. Weinfurter, Phys. Rev. Lett. **85**, 290 (2000).

[27] R. Brouri, A. Beveratos, J. P. Poizat, and P. Grangier, Opt. Lett. **25**, 1294 (2000).

[28] K.-M. C. Fu, C. Santori, P. E. Barclay, I. Aharonovich, S. Prawer, N. Meyer, A. M. Holm, and R. G. Beausoleil, Appl. Phys. Lett. **93**, 234107 (2008).

[29] T. M. Babinec, B. J. M. Hausmann, M. Khan, Y. Zhang, J. R. Maze, P. R. Hemmer, and M. Lončar, Nat. Nanotechnol. **5**, 195 (2010).

[30] A. A. Houck, D. I. Schuster, J. M. Gambetta, J. A. Schreier, B. R. Johnson, J. M. Chow, J. Majer, L. Frunzio, M. H. Devoret, S. M. Girvin, and R. J. Schoelkopf, Nature (London) **449**, 328 (2007).

[31] Stojan Rebić, J. Twamley, and G. J. Milburn, Phys. Rev. Lett. **103**, 150503 (2009).

[32] D. E. Chang, J. I. Cirac, and H. J. Kimble, Phys. Rev. Lett. **110**, 113606 (2013).

[33] M. J. Hartmann, F. G. S. L. Brandao, and M. B. Plenio, Nat. Phys. **2**, 849 (2006).

[34] A. D. Greentre, C. Tahan, J. H. Cole, and L. C. L. Hollenberg, Nat. Phys. **2**, 856 (2006).

[35] D. G. Angelakis, M. F. Santos, and S. Bose, Phys. Rev. A **76**, 031805(R) (2007).

[36] D. G. Angelakis, M. Huo, E. Kyoseva, and L. C. Kwek, Phys. Rev. Lett. **106**, 153601 (2011).

[37] T. Grujic, S. R. Clark, D. Jaksch, and D. G. Angelakis, New J. Phys. **14**, 103025 (2012).

[38] C. Lee, C. Noh, N. Schetakis, and D. G. Angelakis, arXiv:1412.8374.

[39] P. Guimond, A. Roulet, H. N. Le, and V. Scarani, arXiv:1505.07908.

[40] E. Rephaeli and S. Fan, IEEE J. Sel. Top. Quant. **18**, 1754 (2012).

[41] S. Xu and S. Fan, Phys. Rev. A **91**, 043845 (2015).

[42] T. Caneva, M. T. Manzoni, T. Shi, J. S. Douglas, J. I. Cirac, and D. E. Chang, New J. Phys. **17**, 113001 (2015).

[43] H. X. Zheng, D. J. Gauthier, and H. U. Baranger, Phys. Rev. Lett. **111**, 090502 (2013).

[44] H. X. Zheng, D. J. Gauthier, and H. U. Baranger, Phys. Rev. A **85**, 043832 (2012).

[45] H. X. Zheng, D. J. Gauthier, and H. U. Baranger, Phys. Rev. A **82**, 063816 (2010).

[46] D. Roy, Phys. Rev. Lett. **106**, 053601 (2011).

[47] D. Roy, Phys. Rev. A **83**, 043823 (2011).

[48] B. Q. Baragiola, R. L. Cook, A. M. Branczyk, and J. Combes, Phys. Rev. A **86**, 013811 (2012).

[49] M. Pletyukhov and V. Gritsev, Phys. Rev. A **91**, 063841 (2015).

[50] A. J. Miller, S. W. Nam, and J. M. Martinis, and A. V. Sergienko, Appl. Phys. Lett. **83**, 791 (2003).

[51] C. M. Natarajan, M. G. Tanner, and R. H. Hadfield, Supercond. Sci. Technol. **25**, 063001 (2012).

[52] K. D. Irwin and G. C. Hilton, Topics Appl. Phys. **99**, 63 (2005).

[53] E. Rephaeli and S. Fan, Phys. Rev. Lett. **108**, 143602 (2012).

[54] T. Peyronel, O. Firstenberg, Q. Liang, S. Hofferberth, A. V. Gorshkov, T. Pohl, M. D. Lukin, and V. Vuletić, Nature (London) **488**, 57 (2012).

[55] J. F. Huang, T. Shi, C. P. Sun, and F. Nori, Phys. Rev. A **88**, 013836 (2013).

[56] Y. Chang, Z. R. Gong, and C. P. Sun, Phys. Rev. A **83**, 013825 (2011).

[57] J. F. Huang, J. Q. Liao, and C. P. Sun, Phys. Rev. A **87**, 023822 (2013).

[58] M. E. Peskin and D. V. Schroeder, *An Introduction to Quantum Field Theory* (Addison-Wesley, Reading, MA, 1995).

[59] T. Shi and C. P. Sun, arXiv:0907.2776.

[60] C. Zhu, S. Endo, P. Naidon, and P. Zhang, Few-Body Syst. **54**, 1921 (2013).